

1 Biotic and abiotic degradation of the sea ice diatom biomarker IP₂₅ and selected algal sterols
2 in near-surface Arctic sediments

3

4 Jean-François Rontani ^{a*}, Simon T. Belt ^b, Rémi Amiraux ^a

5

6

7 ^a *Aix Marseille University, Université de Toulon, CNRS/INSU/IRD, Mediterranean Institute of*
8 *Oceanography (MIO) UM 110, 13288 Marseille, France*

9

10 ^b *Biogeochemistry Research Centre, School of Geography, Earth and Environmental*
11 *Sciences, University of Plymouth, Drake Circus, Plymouth, Devon PL4 8AA, UK*

12

13

14 * Corresponding author. Tel.: +33-4-86-09-06-02; fax: +33-4-91-82-96-41.

15

16 **ABSTRACT**

17 The organic geochemical IP₂₅ (Ice Proxy with 25 carbon atoms) has been used as a proxy for
18 Arctic sea ice in recent years. To date, however, the role of degradation of IP₂₅ in Arctic
19 marine sediments and the impact that this may have on palaeo sea ice reconstruction based on
20 this biomarker have not been investigated in any detail. Here, we show that IP₂₅ may be
21 susceptible to autoxidation in near-surface oxic sediments. To arrive at these conclusions, we
22 first subjected a purified sample of IP₂₅ to autoxidation in the laboratory and characterised the
23 oxidation products using high resolution gas chromatography–mass spectrometric methods.
24 Most of these IP₂₅ oxidation products were also detected in near-surface sediments collected
25 from Barrow Strait in the Canadian Arctic, although their proposed secondary oxidation and
26 the relatively lower abundances of IP₂₅ in other sediments probably explain why we were not
27 able to detect them in material from other parts of the region. A rapid decrease in IP₂₅
28 concentration in some near-surface Arctic marine sediments, including examples presented
29 here, may potentially be attributed to at least partial degradation, especially for sediment cores
30 containing relatively thick oxic layers representing decades or centuries of deposition. An
31 increase in the ratio of two common phytoplanktonic sterols – epi-brassicasterol and 24-
32 methylenecholesterol – provides further evidence for such autoxidation reactions given the
33 known enhanced reactivity of the latter to such processes reported previously. In addition, we
34 provide some evidence that anaerobic biodegradation processes also act on IP₂₅ in Arctic
35 sediments. The oxidation products identified in the present study will need to be quantified
36 more precisely in downcore records in the future before the effects of degradation processes
37 on IP₂₅-based palaeo sea ice reconstruction can be fully understood. In the meantime, a brief
38 overview of some previous investigations of IP₂₅ in relatively shallow Arctic marine
39 sediments suggests that overlying climate conditions were likely dominant over degradation

40 processes, as evidenced from often increasing IP₂₅ concentration downcore, together with
41 positive relationships to known sea ice conditions.

42

43 *Keywords.* IP₂₅; Sterols; Arctic sediments; Degradation; Autoxidation; Aerobic and anaerobic
44 biodegradation; Palaeo sea ice reconstruction.

45 **1. Introduction**

46 Over the past decade, the Arctic sea ice diatom biomarker IP₂₅ (Ice Proxy with 25
47 carbons atoms; Belt et al., 2007) has emerged as a useful proxy for the past occurrence of
48 seasonal (spring) sea ice when detected in Arctic marine sediments (for a review see Belt and
49 Müller, 2013). Consistent with its origin (i.e., sea ice-associated or sympagic diatoms; Brown
50 et al., 2014), IP₂₅ is a common component of surface sediments across the Arctic (Müller et
51 al., 2011; Stoyanova et al., 2013; Xiao et al., 2013, 2015; Navarro-Rodriguez et al., 2013;
52 Ribeiro et al., 2017; Köseoğlu et al., 2018), while its variability in downcore abundance is
53 generally believed to reflect temporal changes to spring sea ice cover, especially when its
54 concentration profile is considered alongside those of other biomarkers indicative of open-
55 water or ice-edge conditions (e.g., Müller et al., 2009, 2011; Belt et al., 2015), through a
56 combined IP₂₅-phytoplankton biomarker index (PIP₂₅) (Müller et al., 2011), or a multivariate
57 biomarker approach (Köseoğlu et al., 2018). To date, however, the majority of IP₂₅-based
58 studies have focused either on surface sediment analysis or on long-term (multi-centennial or
59 longer) records. Thus, surface sediment analyses have addressed aspects of proxy calibration,
60 generally by comparison of IP₂₅ and other biomarker content with satellite-based
61 measurements of sea ice conditions (Müller et al., 2011; Navarro-Rodriguez et al., 2013;
62 Stoyanova et al., 2013; Xiao et al., 2013, 2015), while temporal studies have concentrated
63 mainly on the reconstruction of sea ice conditions on a multi-centennial scale during the
64 Holocene (e.g., Vare et al., 2009; Belt et al., 2010; Müller et al., 2012; Berben et al., 2014,
65 2017; Hörner et al., 2016, 2017; Stein et al., 2017), recent glacial/interglacial intervals (Müller
66 et al., 2014; Hoff et al., 2016), the Mid-Pleistocene Transition (Detlef et al., 2018), and even
67 longer timeframes extending back to the Pliocene/Pleistocene boundary and the late Miocene
68 (Stein and Fahl, 2013; Knies et al., 2014; Stein et al., 2016). One key attribute of IP₂₅ as a sea
69 ice proxy is its apparent relative stability in sediments. Indeed, the identification of IP₂₅ in

70 sediments several million years old (Knies et al., 2014; Stein et al., 2016) has been attributed,
71 in part, to such stability, and is supported by laboratory-based investigations, where it has
72 been shown to be significantly less reactive towards degradation process such as photo-
73 oxidation and autoxidation, at least compared to other common phytoplanktonic lipids
74 (Rontani et al., 2011, 2014). As such, sedimentary signals have been interpreted as reflecting
75 climatic (sea ice) conditions rather than diagenetic artefacts, although the possibility of some
76 diagenetic over-printing of the environmental signal has been noted (e.g., Belt and Müller,
77 2013; Polyak et al., 2016). In contrast, temporal investigations covering recent decades or
78 centuries are less common, although some studies from North Iceland (Massé et al., 2008;
79 Andrews et al., 2009), East Greenland (Alonso-García et al., 2013; Kölling et al., 2017), the
80 Barents Sea (Vare et al., 2010; Köseoğlu et al., 2018), northern Baffin Bay (Cormier et al.,
81 2016) and the Chukchi-Alaskan margin (Polyak et al., 2016) have been reported. Such studies
82 are somewhat different from those carried out on surface sediments (typically 0–1 cm) or
83 longer timeframe investigations generally conducted on material from gravity/piston cores
84 since, in some cases, at least, they likely result from analysis of material that spans the
85 oxic/anoxic (redox) sediment boundary. However, such boundary layers are not generally
86 identified (reported), even though they are likely found in the upper few centimetres of box
87 cores or multi-cores, which reflect accumulation over decades or recent centuries for many
88 Arctic Shelf regions (e.g., Stein and Fahl, 2000; Darby et al., 2006; Mudie et al., 2006; Maiti
89 et al., 2010; Vare et al., 2010). On the other hand, in the central Arctic Ocean, such a layer
90 may reflect substantially longer-term accumulation due to much lower sedimentation rates
91 (e.g., Stein et al., 1994a,b).

92 The rate and extent of degradation of sedimentary organic compounds is strongly
93 dependent on the molecular structure of the substrate, protective effects offered by association
94 of organic matter with particle matrices, and the length of time accumulating particles are

95 exposed to molecular oxygen in sedimentary pore waters (Henrich, 1991; Hartnett et al.,
96 1998). The main degradative processes in the oxic layer of sediments are aerobic
97 biodegradation and autoxidation. Numerous organisms, including bacteria, fungi and micro-
98 and macrofauna, are responsible for the aerobic biodegradation of organic carbon in
99 sediments (Fenchel et al., 1998) and almost all of these organisms have the enzymatic
100 capacity to perform a total mineralization of numerous organic substrates (Kristensen, 2000).
101 Although autoxidation of organic matter involving spontaneous free radical reaction of
102 organic compounds with O₂ has been rather under-considered in the marine realm, it is now
103 known that autoxidative processes can act very intensively on vascular plant debris in Arctic
104 sediments (Rontani et al., 2017). This high autoxidation efficiency likely reflects the enhanced
105 photooxidation of senescent vascular plants in the region (thus yielding high amounts of
106 hydroperoxides), together with high lipoxygenase activity (a potential source of radicals;
107 Fuchs and Spiteller, 2014). Indeed, the latter mechanism has recently been observed in
108 sinking particles dominated by ice algae (Amiriaux et al., 2017) and in particles discharged
109 from the Mackenzie River (Galeron et al., 2017).

110 The principal aim of the current study, therefore, was to investigate whether we could
111 provide evidence for oxidative degradation processes acting on IP₂₅ in near-surface Arctic
112 sediments and thus, potentially, on any resultant palaeo sea ice reconstructions. To achieve
113 this, we first carried out laboratory-based oxidation of purified IP₂₅ and carried out product
114 identification using high resolution mass spectral analysis. Since IP₂₅ was shown previously
115 to be relatively resistant to oxidation (Rontani et al., 2014), more powerful oxidizing
116 conditions were used. We then investigated the occurrence of the same oxidation products in
117 sediment samples taken from box cores retrieved from three regions of the Canadian Arctic.
118 To complement the IP₂₅-based findings, we also measured the ratios of two common algal
119 sterols – epi-brassicasterol and 24-methylenecholesterol – to provide further evidence of

120 different oxidative pathways under oxic and anoxic conditions. Geochemical analysis of the
121 box cores revealed variable redox boundary depths, which provided further context for
122 interpreting the biomarker data.

123

124 **2. Experimental**

125 *2.1. Sediment and sea ice algal sampling*

126 Investigations of in situ degradation processes were performed on sediment material
127 and sea ice algal aggregates. Sediment material was obtained from three locations within the
128 Canadian Arctic Archipelago (CAA) on board the CCGS Amundsen in 2005 and 2007 (Vare
129 et al., 2009; Belt et al., 2010; 2013). Sampling locations correspond to Barrow Strait (STN 4),
130 Viscount Melville Sound (STN 308) and the western Amundsen Gulf (STN 408) (Fig. 1). In
131 each case, box cores were collected, sectioned on board, with sub-samples (1 cm resolution)
132 then being freeze-dried before storage between $-20\text{ }^{\circ}\text{C}$ and $+4\text{ }^{\circ}\text{C}$ prior to analysis. Regular
133 monitoring of IP_{25} concentration in these sediments stored under such conditions (since their
134 collection) has not revealed any significant degradation (i.e. $< 10\%$; Cabedo-Sanz et al.,
135 2016). Previous reports of sedimentation rates from the study area (e.g., 0.15 cm/yr for the
136 Barrow Strait (STN 4) core (Belt et al., 2010)) and preliminary additional ^{210}Pb data (S.
137 Schmidt, personal communication) suggest that box cores (ca. 20 cm) from the region
138 typically represent decades to centuries of accumulation. A sample of floating sea ice algal
139 aggregates was obtained from Resolute Passage (western Barrow Strait) in 2012 as described
140 by Brown et al. (2014).

141 Redox boundary layers in each of the box cores were identified using the change
142 (reduction) in Mn content as described previously (Vare et al., 2009; Brown, 2011 and
143 References cited therein). Using this approach, redox boundaries were identified at ca. 2 cm in
144 the box core from Barrow Strait (STN 4) and at ca. 11 cm and ca. 8 cm in box cores from

145 Viscount Melville Sound (STN 308) and the western Amundsen Gulf (STN 408), respectively
146 (L. Vare, personal communication).

147

148 2.2. *IP₂₅ isolation*

149 A sample of *IP₂₅* (ca. 99%) was obtained by extraction of a multi-kg quantity of
150 sediment from Barrow Strait in the Canadian Arctic (STN 4; Fig. 1) and purification by a
151 combination of open column chromatography (SiO_2 ; hexane) and Ag^+ HPLC as described
152 previously in detail by Belt et al. (2012).

153

154 2.3. *Production of *IP₂₅* oxidation products*

155 All procedures were carried out on a ca. 10–50 μg scale. Oxidation of *IP₂₅* using RuCl_3
156 and *tert*-butyl hydroperoxide in cyclohexane at room temperature for 16 h (Seki et al., 2008)
157 produced 3,9,15-trimethyl-6-(1,5-dimethylhexyl)-tetradec-1-en-3-ol (**1**) and 3,9,15-trimethyl-
158 6-(1,5-dimethylhexyl)-tetradec-2-en-1-ol (**2**) with yields of 5% and 2%, respectively.

159 OsO_4 oxidation of *IP₂₅* in anhydrous dioxane/pyridine (McCloskey and McClelland,
160 1965) afforded 3,9,15-trimethyl-6-(1,5-dimethylhexyl)-tetradecan-1,2-diol (**6**) as the major
161 product (ca. 45%) together with smaller amounts of 2,8,12-trimethyl-5-(1,5-dimethylhexyl)-
162 tridecanoic acid (**7**) (ca. 6%) resulting from diol cleavage and subsequent oxidation of the
163 aldehyde thus formed.

164 The structures of all *IP₂₅* oxidation products are shown in the Appendix. Due to the
165 very low amounts of *IP₂₅* available, compounds **1**, **2**, **6** and **7** could not be produced in
166 sufficient amounts to permit quantification, although comparison of their mass spectra and
167 retention times with compounds detected in sediments confirmed their identification.

168

169 2.4. *Induction of autoxidation in solvent*

170 Autoxidation experiments were performed under an atmosphere of air in 15 ml screw-
171 cap flasks containing IP₂₅ (10 µg), *tert*-butyl hydroperoxide (200 µl of a 6.0 M solution in
172 decane), di-*tert*-butyl nitroxide (1.2 mg) and hexane (2 ml). After stirring, the flask was
173 incubated in the dark at 65 °C. A relatively high temperature was selected in order to
174 accelerate the autoxidation reactions. Aliquots (200 µl) were withdrawn from the reaction
175 mixture after incubation for different times. Each sub-sample was evaporated to dryness under
176 a stream of nitrogen and analyzed by gas chromatography–electron ionization quadrupole
177 time of flight mass spectrometry (GC–QTOFMS) after NaBH₄ reduction (see Section 2.5) and
178 derivatization (see Section 2.8) for identification of hydroxylated oxidation products.

179

180 *2.5. Reduction of oxidation products*

181 Hydroperoxides resulting from IP₂₅ oxidation were reduced to the corresponding
182 alcohols by reaction with excess NaBH₄ in diethyl ether:methanol (4:1, v:v, 10 mg/mg of
183 residue) at room temperature (1 h). After reduction, a saturated solution of NH₄Cl (10 mL)
184 was added cautiously to remove any unreacted NaBH₄. The pH was then adjusted to 1 with
185 dilute HCl (2 N) and the mixture shaken and extracted with hexane:chloroform (5 ml, 4:1,
186 v:v; ×3). The combined extracts were dried over anhydrous Na₂SO₄, filtered and evaporated
187 to dryness under a stream of nitrogen.

188

189 *2.6. Aerobic biodegradation of phytoplankton sterols*

190 Aerobic biodegradation of phytoplankton cells was performed using the upper layer
191 (0–1 cm) of Arctic sediments collected in July 2016 from Davis Strait (70°29'55.56" N,
192 59°31'30.24" W) during the GreenEdge cruise on board the CCGS Amundsen as bacterial
193 inoculum. Enrichment cultures were incubated in the dark in 250 ml Erlenmeyer flasks
194 containing 50 ml portions of an enrichment medium consisting of LB medium (20 ml) and

195 phytoplankton suspension (10 ml) (10 mg dry weight) as carbon source. Samples were
196 maintained at 2 °C (a temperature close to that of Arctic waters) and agitated using a
197 reciprocal shaker for different times. The amounts of 24-methylenecholesterol and epi-
198 brassicasterol in the sediment inoculum were negligible relative to those in the phytoplankton
199 suspension. These phytoplankton cells (mainly composed of diatoms) were collected in
200 Commonwealth Bay (East Antarctica, 66°56'S; 142°27'E) during the IPEV-COCA2012 cruise
201 in January 2012 as described previously (Rontani et al., 2014). After incubation,
202 phytoplankton material was recovered by filtration on GF/F filters and saponified as described
203 in Section 2.7.

204

205 *2.7. Sediment and sea ice algal treatment*

206 Sediments from box cores (i.e., STN 4, 308, 408) or sea ice algae (19.3 mg dry
207 weight) were placed in MeOH (15 ml) and hydroperoxides were reduced to the corresponding
208 alcohols with excess NaBH₄ (70 mg, 30 min at 20 °C). Following the reduction step, water
209 (15 ml) and KOH (1.7 g) were added and the mixture saponified by refluxing (2 h). After
210 cooling, the contents of the flask were acidified with HCl to pH 1 and extracted three times
211 with dichloromethane (DCM) (30 ml). The combined DCM extracts were dried over
212 anhydrous Na₂SO₄, filtered and concentrated to give a total lipid extract (TLE). Since IP₂₅
213 oxidation product content was quite low relative to other lipids, accurate quantification
214 required further separation of the TLE using column chromatography (silica; Kieselgel 60, 8
215 cm × 0.5 cm i.d.). IP₂₅ was obtained by elution with hexane (10 ml) and its oxidation products
216 by subsequent elution with DCM (10 ml). Additional elution with MeOH (10 ml) was carried
217 out to recover the more polar lipid compounds. Relative IP₂₅ content was determined using
218 the method of Vare et al. (2009) and Belt et al. (2010) and some uncalibrated data (STN 308)
219 were presented previously by Brown (2011). Here, all previous GC–MS data were re-

220 analysed and converted to absolute concentrations using instrumental response factors derived
221 from solutions of known IP₂₅ concentration (Belt et al., 2012). Biomarker data were further
222 normalised to total organic carbon (TOC) to accommodate possible changes in burial
223 efficiency. TOC data were obtained following removal of inorganic carbonate from sediment
224 material according to the method of Berben et al. (2017).

225

226 *2.8. Derivatization of hydroxyl-containing products*

227 In order to analyse for hydroxylated products (i.e. alcohols and carboxylic acids),
228 DCM- and MeOH-eluted fractions were derivatized by dissolving them in 300 µl
229 pyridine/*bis*-(trimethylsilyl)trifluoroacetamide (BSTFA; Supelco; 2:1, v:v) and silylated (50
230 °C, 1 h). After evaporation to dryness under a stream of N₂, the derivatized residue was re-
231 dissolved in 100 µl BSTFA (to avoid desilylation of fatty acids), together with an amount of
232 co-solvent (ethyl acetate) dependent on the mass of the TLE, and then analyzed using GC-
233 QTOFMS.

234

235 *2.9. GC-QTOFMS analyses*

236 Accurate mass spectra were obtained with an Agilent 7890B/7200 GC-QTOFMS
237 System (Agilent Technologies, Parc Technopolis - ZA Courtaboeuf, Les Ulis, France). A
238 cross-linked 5% phenyl-methylpolysiloxane (Macherey Nagel; Optima 5-MS Accent) column
239 (30 m × 0.25 mm, 0.25 µm film thickness) was employed. Analysis was performed with an
240 injector operating in pulsed splitless mode at 280 °C and the oven temperature programmed
241 from 70 °C to 130 °C at 20 °C/min, then to 250 °C at 5 °C/min and then to 300 °C at 3
242 °C/min. The carrier gas (He) was maintained at 0.69×10^5 Pa until the end of the temperature
243 program. Instrument temperatures were 300 °C for transfer line and 230 °C for the ion source.
244 Accurate mass spectra were recorded across the range m/z 50–700 at 4 GHz with nitrogen as

245 collision gas (1.5 ml/min). The QTOFMS instrument provided a typical resolution ranging
246 from 8009 to 12252 from m/z 68.9955 to 501.9706. Perfluorotributylamine (PFTBA) was
247 utilized for daily MS calibration. Structural assignments were based on interpretation of
248 accurate mass spectral fragmentations and confirmed by comparison of retention times and
249 mass spectra of oxidation products with those of authentic compounds, when available.

250

251 **3. Results**

252 *3.1. Autoxidation and biodegradation rates of epi-brassicasterol, 24-methylenecholesterol* 253 *and IP₂₅*

254 Autoxidation rates of 24 α -methylcholesta-5,22E-dien-3 β -ol (epi-brassicasterol) and
255 24-methylcholesta-5,24(28)-dien-3 β -ol (24-methylenecholesterol) were previously measured
256 in phytoplankton cells (Rontani et al., 2014). In order to compare biodegradation rates of
257 these two sterols, phytoplanktonic cells were incubated in the presence of sediment inoculum
258 under oxic conditions. We observed a strong depletion of both sterols (close to 90% after
259 incubation for 1 month at 2 °C), although their biodegradation rates were quite similar (Table
260 1). The pseudo-first order rate constant (k) for the biodegradation of each sterol was obtained
261 from the gradient of the regression lines determined according to the relationship $\ln(C/C_0) = -$
262 kt , where C is the concentration of an analyte at the time of sampling, C₀ is the initial
263 concentration, and t corresponds to the duration of the incubation. For these experiments, a
264 microbially mediated change in the sterol content is supported by the near invariance of the
265 concentration of 24-ethylcholesta-3 β ,5 α ,6 β -triol, a well-known autoxidation product of
266 sitosterol (Rontani et al., 2009).

267 Incubation of hexane solutions of IP₂₅ in the presence of *tert*-butyl hydroperoxide and
268 di-*tert*-butyl nitroxide at 65 °C, with subsequent NaBH₄-reduction and silylation, yielded
269 several HBI alcohol TMS derivatives (resulting from the reduction and the silylation of the

270 corresponding, hydroperoxides, respectively) that could be identified by GC–QTOFMS.
271 Specifically, the formation of 3,9,15-trimethyl-6-(1,5-dimethylhexyl)-tetradec-1-en-3-ol (**1**)
272 and 3,9,15-trimethyl-6-(1,5-dimethylhexyl)-tetradec-2-en-1-ol (**2**) was supported by
273 comparison of their accurate mass spectra (Fig. 2A) and retention times with those of
274 reference compounds prepared by oxidation of purified IP₂₅ (see Section 2.3). Furthermore,
275 2,6,10,14-tetramethyl-9-(3-methylpent-4-enyl)-pentadecan-2-ol (**3**), 2,6,10,14-tetramethyl-7-
276 (3-methylpent-4-enyl)-pentadecan-2-ol (**4**) and 2,6,10,14-tetramethyl-9-(3-methylpent-4-
277 enyl)-pentadecan-6-ol (**5**) could be tentatively identified on the basis of their accurate mass
278 fragmentations (Fig. 2B and 2C).

279

280 *3.2. Degradation of IP₂₅, epi-brassicasterol and 24-methylenecholesterol in Arctic sediments*

281 IP₂₅ concentrations (Supplementary Table S1) and the ratio epi-brassicasterol/24-
282 methylenecholesterol (Bra/24-Me) were monitored in the upper sections (up to ca. 20 cm) of
283 three short sediment cores collected from different regions of the Canadian Arctic, which
284 possessed contrasting near-surface redox properties. Thus, sediments from Viscount Melville
285 Sound (STN 308) and the western Amundsen Gulf (STN 408) exhibited a thick oxic layer (11
286 cm and 8 cm, respectively), while the redox boundary was much shallower (ca. 2 cm) in the
287 box core from Barrow Strait (STN 4). After an increase in the first 3 cm, IP₂₅ concentration
288 (expressed relative to TOC) decreased substantially in the 3–11 cm sections of (oxic)
289 sediments from Viscount Melville Sound (STN 308). Similarly, a reduction in IP₂₅
290 concentration was identified in the top 3 cm of oxic sediments from the western Amundsen
291 Gulf (STN 408) before a subsequent increase (ca. 3–11 cm) and then decrease (Fig. 3). In
292 contrast, IP₂₅ concentration remained relatively constant in the case of Barrow Strait (STN 4)
293 sediments (Fig. 3). Concerning the two main sterols, the ratio Bra/24-Me remained relatively
294 constant in anoxic sediments from Barrow Strait (STN 4), although it increased steadily in

295 oxic sediments from Viscount Melville Sound (STN 308) (Fig. 3). Sediments from the
296 western Amundsen Gulf (STN 408), Bra/24-Me increased strongly in the first 4 cm, before
297 decreasing and then stabilizing (Fig. 3).

298 Next, we aimed to identify IP₂₅ autoxidation products in the DCM fractions of the
299 TLEs of different sediments by comparison of accurate mass fragmentations and retention
300 times with the oxidation products characterised during the thermal incubation reactions. Using
301 this approach, we detected compounds **1**, **3**, **4** and **5** in sediments from Barrow Strait (STN 4),
302 which also contained the highest concentrations of IP₂₅ (Fig. 4). The combined relative
303 abundance of these compounds (estimated on the basis of similar TOFMS responses to that of
304 IP₂₅) reached 8.8% of the amount of IP₂₅ in the 1–2 cm layer and then decreased rapidly to
305 1.2% in the 3–4 cm horizon. In addition, 2,6,10,14-tetramethyl-7-(3-methylpenten-4-yl)-
306 pentadecan-6-ol (**8**), which was absent in the incubation experiments, was also identified,
307 albeit tentatively (Fig. 4B). In contrast, since the mass spectrum of the TMS derivative of the
308 saturated tertiary C₂₅ HBI alcohol (C-7) had already been reported (Robson, 1987), we were
309 able to investigate if the corresponding mono-unsaturated oxidation product was also present;
310 however, no characteristic fragmentation ions corresponding to oxidation at C-7 of IP₂₅ could
311 be identified. Analysis of extracts by GC–QTOFMS did, however, enable us to detect 3,9,15-
312 trimethyl-6-(1,5-dimethylhexyl)-tetradecan-1,2-diol (**6**) in sediments from Barrow Strait (STN
313 4) and the western Amundsen Gulf (STN 408) (Fig. 5), while traces of 2,8,12-trimethyl-5-
314 (1,5-dimethylhexyl)-tridecanoic acid (**7**) could be identified in Barrow Strait (STN 4) and
315 Viscount Melville Sound (STN 308) sediments (Fig. 6). These two compounds were formally
316 identified by comparison of their accurate mass spectra (Fig. 7) and retention times with those
317 of standards. On the other hand, we failed to detect compounds **1-8** in floating sea ice algal
318 aggregates from Resolute Passage despite the presence of relatively large amounts of IP₂₅
319 within these samples (Brown et al., 2014).

320

321 **4. Discussion**

322 *4.1. Autoxidation of IP₂₅*

323 According to our product identifications, autoxidation of IP₂₅ involves hydrogen atom
324 abstraction by peroxy radicals on the allylic carbon C-22 and the tertiary carbon atoms C-2,
325 C-10 and C-14. Subsequent oxidation of the resulting radicals together with hydrogen
326 abstraction from other substrate molecules leads to the formation of various hydroperoxides
327 (Fig. 8). These labile compounds were reduced to their corresponding alcohols (**1-5**) during
328 NaBH₄-reduction and silylated prior to analysis by GC-QTOFMS. The failure to detect any
329 autoxidation product resulting from reaction with either of the tertiary carbons C-6 or C-7 is
330 likely due to increased steric hindrance during hydrogen abstraction by the bulky *tert*-
331 butylperoxy radicals employed during the incubation. Indeed, when comparing our data from
332 laboratory and environmental samples, we note that the relative abundances of IP₂₅ oxidation
333 products are very different in Arctic sediments (Fig. 4B) compared to those from incubations
334 in solvent (Fig. 4A), likely reflecting the contrasting nature of the peroxy radicals involved
335 during autoxidation. For example, the bulky *tert*-butylperoxy radical pertinent to the
336 laboratory-based incubations probably favours the attack of the less hindered external carbon
337 atoms of IP₂₅ (i.e. C-2 and C-14), while the unknown (structurally) peroxy radicals acting in
338 sediment seem to be less sensitive to such steric hindrance. This conclusion is further
339 supported by the detection of an additional oxidation product in sediments (Fig. 4B),
340 tentatively attributed to 2,6,10,14-tetramethyl-7-(3-methylpenten-4-yl)-pentadecan-6-ol (**8**),
341 which was absent in the incubation experiments (Fig. 4A).

342 Finally, although each of **1-5** could be readily identified during the incubation
343 reactions, they were only ever present in low abundances and none accumulated over time.
344 We attribute this to the likely secondary oxidation of primary hydroperoxides to polar and

345 oligomeric compounds (Fig. 8), which are not detectable using the GC–QTOFMS method
346 employed here. This kind of secondary oxidation was described previously for other HBIs
347 (Rontani et al., 2014).

348

349 *4.2. Degradation of epi-brassicasterol and 24-methylenecholesterol*

350 Due to the different positions of the double bonds in their alkyl chains (see Appendix),
351 an enhanced autoxidative and photooxidative reactivity of epi-brassicasterol compared to 24-
352 methylenecholesterol would be expected. Indeed, the C-H bond energy for allylic hydrogens
353 is lower for internal double bonds than it is for terminal double bonds (77 kcal/mole vs 85
354 kcal/mole) (Schaich, 2005), thus making allylic hydrogen abstraction more favourable in epi-
355 brassicasterol. Moreover, on the basis of degradation rates of singlet oxygen ($^1\text{O}_2$) with
356 terminal and internal double bonds (4.0×10^3 and $7.7 \times 10^3 \text{ M}^{-1} \text{ s}^{-1}$, respectively; Hurst et al.,
357 1985), Type II photosensitized oxidation of epi-brassicasterol should also be favoured
358 compared to 24-methylenecholesterol. However, in natural settings, it was previously reported
359 that autoxidation (Rontani et al., 2014) and photooxidation (Rontani et al., 2012; 2016)
360 processes act more intensively on 24-methylenecholesterol than on epi-brassicasterol, at least
361 in mixed phytoplanktonic assemblages. These differences in reactivity can be attributed to the
362 involvement of intra-cellular compartmentalization effects, which may significantly modify
363 the reactivity of lipids towards autoxidative and photooxidative processes according to their
364 location in phytoplanktonic cells (Rontani, 2012). This enhanced reactivity of 24-
365 methylenecholesterol towards autoxidation in phytoplanktonic cells suggests that an increase
366 in the Bra/24-Me ratio may be a good indicator of autoxidation processes in sediments,
367 especially as the main autoxidative products of these two sterols are unspecific and labile
368 $7\alpha/\beta$ -hydroperoxysteroids (Christodoulou et al., 2009; Rontani et al., 2009).

369 In contrast to autoxidation reactions, aerobic microbial degradation of Δ^5 -sterols
370 involves two processes: side-chain elimination and ring opening (Rostoniec et al., 2009). The
371 degradation is initiated by oxidation of the 3β -hydroxyl moiety and isomerization of the Δ^5
372 double bond to the Δ^4 position (Sojo et al., 1997). Further degradation of the resulting 4-
373 steren-3-one proceeds via hydroxylation at C₂₆ to initiate side-chain degradation, or oxidation
374 of rings A and B resulting in the cleavage of the ring structure (9,10-seco-pathway; Philipp,
375 2011). In the case of cholesterol, the degradation of the 26-hydroxylated alkyl chain may be
376 carried out after oxidation to the corresponding acid by classical sequences of β -oxidation
377 (Rostoniec et al., 2009). In contrast, in the case of epi-brassicasterol and 24-
378 methylenecholesterol, due to the presence of a methyl or methylene group at C-24, the
379 involvement of alternating β -decarboxymethylation (Cantwell et al., 1978) and β -oxidation
380 sequences is needed (Fig. 9). The very close degradation rates of these two sterols observed
381 after incubation of phytoplanktonic cells in the presence of sediment inoculum under oxic
382 conditions (Table 1) may be attributed to the involvement of a 2,3-enoyl-CoA isomerase
383 (Ratledge, 1994). Indeed, these widely distributed enzymes may catalyze the isomerisation of
384 the methylidene double bond to the C24-25 position in the case of 24-methylenecholesterol
385 (Fig. 9), thus permitting the involvement of a similar degradation process of the alkyl side-
386 chain in the case of the two sterols.

387 Under anoxic conditions, ring cleavage of Δ^5 -sterols may be mediated by oxygen-
388 independent enzymatic processes (Chiang et al., 2007). In the case of cholesterol, only
389 hydroxylation of the side chain at C-25 has been shown to occur, with the resulting tertiary
390 alcohol not oxidized further (Chiang et al., 2007). For sterols with more substituted or
391 unsaturated side chains, such as sitosterol, fucosterol and isofucosterol, similar degradation
392 rates were observed following incubation of cells of the microalga *Nannochloropsis salina* in
393 anoxic sediment slurries (Grossi et al., 2001). This suggests that changes to the sterol side

394 chain have little impact on the overall degradation rates under anoxic conditions. As such, in
395 the absence of any reported experimental data, it is reasonable to propose similar anaerobic
396 degradation rates for epi-brassicasterol and 24-methylenecholesterol, especially given their
397 common ring structure. Overall, therefore, aerobic and anaerobic bacterial degradation
398 processes should not induce significant changes to the Bra/24-Me ratio in sediments.

399

400 *4.3. Degradation of IP₂₅, epi-brassicasterol and 24-methylenecholesterol in Arctic sediments*

401 Due to the extremely low rate of autoxidation of IP₂₅ in solution, even at higher
402 temperature (e.g., 65 °C), it was suggested previously that it should be largely unaffected by
403 autoxidative degradation processes in the Arctic, at least in comparison with lipids of similar
404 structure such as other HBIs with greater unsaturation (Rontani et al., 2014). However, here
405 we show that autoxidative degradation of IP₂₅ may occur under more ‘forced’ conditions and
406 such processes may also take place in Arctic surface sediments. Indeed, due to recent
407 evidence of strong lipoxygenase activity (a well-known source of radicals; Fuchs and
408 Spiteller, 2014) in bacteria associated with ice algae (Amiriaux et al., 2017) and in terrestrial
409 particulate organic matter discharged from Arctic rivers (Galeron et al., 2017), autoxidative
410 degradation reactions can even be dominant in Arctic sediments (Rontani et al., 2012; 2017),
411 despite the low temperatures. The autoxidation of IP₂₅ in sediments possessing a thick oxic
412 layer, where the contact of ice algal detritus with oxygen may be relatively long, therefore
413 represents a viable degradation pathway of this biomarker in near-surface sediments.

414 Consistent with this suggestion, the decrease in IP₂₅ concentration observed in the oxic
415 layer of sediments from Viscount Melville Sound (STN 308) (between 3 and 10 cm) and the
416 western Amundsen Gulf (STN 408) (between 0 and 3 cm) (Fig. 3) may potentially be
417 attributed to the involvement of oxic degradation processes such as aerobic biodegradation
418 (Robson and Rowland, 1988) or autoxidation, and this last suggestion is supported further by

419 the increase of the Bra/24-Me ratio within the same sediments (Fig. 3). In contrast, the strong
420 decrease in Bra/24-Me observed in the bottom of the oxic layer of sediments from the western
421 Amundsen Gulf (STN 408) is potentially due to an input of fresh algal material (with a low
422 Bra/24-Me ratio) during this period. This suggestion is supported by the observation of a 10-
423 fold increase in phytoplanktonic sterol concentration in the 6–7 cm horizon compared to the
424 4–5 cm layer. Further, Brown (2011) proposed that rapid decreases in sedimentary IP₂₅
425 concentration in some other cores from the Canadian Arctic could potentially reflect
426 degradation processes, more generally. In contrast, the more consistent concentration of IP₂₅
427 in anoxic sediments from Barrow Strait (STN 4) and the western Amundsen Gulf (STN 408)
428 (Fig. 3) is likely indicative of enhanced resistance to oxidation under such conditions.
429 Unfortunately, we were not able to detect the primary autoxidation products of IP₂₅ in
430 sediments other than from Barrow Strait (STN 4), likely due to: (i) their further oxidation (as
431 suggested from the incubation reactions), especially in the oxic layers of cores from Viscount
432 Melville Sound (STN 308) and the western Amundsen Gulf (STN 408) and (ii) the detection
433 limits of GC–QTOFMS analyses. However, despite the general resistance of IP₂₅ towards free
434 radical oxidation, as reported previously (Rontani et al., 2011, 2014), the detection of
435 compounds **1**, **3**, **4** and **5** (Fig. 4) shows that this HBI alkene can be susceptible to
436 autoxidation in Arctic sediments, an environment where such processes have previously been
437 shown to be enhanced for some other lipids (Rontani et al., 2012; 2017). Further, this
438 vulnerability towards autoxidation may be especially prevalent in cases where sequestered ice
439 algal material experiences long residence times in the oxic layer.

440 Interestingly, compounds **6** and **7** could be detected in anoxic sediments from Barrow
441 Strait (STN 4) and oxic sediments from Viscount Melville Sound (STN 308) and the western
442 Amundsen Gulf (STN 408) (Figs. 5 and 6). We attribute the formation of such compounds to
443 aerobic or anaerobic bacterial metabolism of IP₂₅. In contrast, a mechanism involving

444 autoxidative production (via epoxidation and subsequent hydrolysis; Schaich, 2005) is
445 discarded on the basis of: (i) the detection of only one pair of enantiomers of compound **6** in
446 sediments (Fig. 5) and (ii) the lack of compounds **6** and **7** observed during our in vitro
447 autoxidation experiments. Aerobic bacterial degradation of IP₂₅ may be initiated either via
448 attack on the double bond or by the same mechanisms associated with *n*-alkane metabolism
449 (i.e., attack of terminal methyl groups; Morgan and Watkinson, 1994). Oxidation across the
450 double bond in IP₂₅ can produce diol **6** via the corresponding epoxide **9** (Soltani et al., 2004)
451 (Fig. 10). Previously, it was demonstrated that various pristenes and phytene (also isoprenoid
452 alkenes) can be rapidly biodegraded by sedimentary bacteria under anaerobic conditions,
453 mainly by hydration reactions (Rontani et al., 2013). Enzymes that catalyze the addition of
454 water to isolated and electron-rich carbon-carbon double bonds are termed hydratases and
455 display a high degree of enantioselectivity (Resch and Hanefeld, 2015). In the case of IP₂₅,
456 addition of water to the C23-24 double bond results in the formation of 3,9,15-trimethyl-6-
457 (1,5-dimethylhexyl)-tetradecan-2-ol (**10**) (Fig. 10), which subsequently oxidises to the
458 corresponding ketone (**11**). Mechanisms involving hydration of the enol forms of the keto
459 group have been proposed for the anaerobic metabolism of isoprenoid ketones by denitrifiers
460 (Rontani et al., 1999; 2013). Hydration of the enol form under kinetic control of the ketone **11**
461 affords the diol **6** (Fig. 10). This diol may be subsequently cleaved to form 2,8,12-trimethyl-5-
462 (1,5-dimethylhexyl)-tridecanal (**12**), which may then be fully metabolized via 2,8,12-
463 trimethyl-5-(1,5-dimethylhexyl)-tridecanoic acid (**7**) by alternating β -oxidation and β -
464 decarboxymethylation sequences (Cantwell et al., 1978; Rontani and Volkman, 2003). These
465 interesting results suggest that IP₂₅ may be also affected by bacterial degradation processes in
466 Arctic sediments, although the extent to which this occurs remains to be determined.

467

468 *4.4. Implications for palaeo sea ice reconstruction*

469 The identification of some degradation pathways of IP₂₅ in some Arctic marine
470 sediments raises potentially important questions regarding the use of this biomarker as a
471 reliable proxy measure of past sea ice. However, the failure to investigate the occurrence of
472 any of the degradation products described herein in previous studies, prevents a
473 comprehensive evaluation of the importance of IP₂₅ degradation from being made at this
474 stage. In the meantime, analysis of an extensive set of surface sediments from different Arctic
475 regions has revealed excellent agreement between IP₂₅ content and known sea ice cover (e.g.,
476 Müller et al., 2011; Stoyanova et al., 2013; Navarro-Rodriguez et al., 2013; Xiao et al., 2013,
477 2015; Belt et al., 2015; Köseoğlu et al., 2017; Ribeiro et al., 2017), while IP₂₅ data obtained
478 from several short core records (typically covering recent decades to centuries) show
479 generally good agreement with known sea ice conditions derived either from historical
480 records or satellite data (Alonso-García et al., 2013; Weckström et al., 2013; Cormier et al.,
481 2016), including examples where IP₂₅ even increases with depth (e.g., Massé et al., 2008;
482 Andrews et al., 2009; Vare et al., 2010; Cabedo-Sanz and Belt, 2016). However, in a recent
483 study from the Chukchi-Alaskan margin, a decline in IP₂₅ abundance in near-surface
484 sediments was suggested to indicate a combined influence of diagenesis and long-range
485 sediment transport (Polyak et al., 2016). Further, the previously reported surface sediment
486 datasets (and their relationship to known sea ice cover) might need re-examination in light of
487 the evidence described herein for at least partial IP₂₅ degradation in some near-surface
488 sediments.

489 Interestingly, although there is a clear decline in IP₂₅ concentration with depth in the
490 box core from Viscount Melville Sound (STN 308) (Fig. 3), a similarly continuous negative
491 trend was not apparent in the cores from either Barrow Strait (STN 4) or the western
492 Amundsen Gulf (STN 408) (Fig. 3), despite the detection of IP₂₅ oxidation products in both
493 cases (Fig. 5D). This suggests that climatic influences likely exceeded those from

494 degradation, although the possible impact of bioturbation, a feature in some near-surface
495 sediments, cannot be totally ruled out at this stage. However, preliminary ^{210}Pb data suggest
496 that bioturbation is negligible in cores from Barrow Strait (STN4) and Viscount Melville
497 Sound (STN308), and confined to the (at most) upper 2 cm in the core from the western
498 Amundsen Gulf (STN408) (S. Schmidt, personal communication).

499 For longer records (i.e. those beyond recent centuries), a common feature in many
500 IP_{25} -based sea ice reconstructions has been a reduction in IP_{25} concentration over time,
501 especially during the Holocene (e.g., Vare et al., 2009; Belt et al., 2010, Fahl and Stein, 2012;
502 Müller et al., 2012, Hörner et al., 2016; Kölling et al., 2017; Stein et al., 2017). Such changes
503 have generally been interpreted as reflecting an increase in sea ice extent or duration from the
504 warm early Holocene through neoglacial conditions towards present, an interpretation
505 generally supported with other paleoclimatic proxy data. The often higher IP_{25} concentrations
506 observed in older sections of the same (or related) records, covering the Younger Dryas
507 stadial (ca. 12.9–11.5 kyr BP) (Cabedo-Sanz et al., 2013, Müller and Stein, 2014; Belt et al.,
508 2015; Méheust et al., 2015; Jennings et al., 2017; Xiao et al., 2017) and the Last Glacial
509 Maximum (LGM; e.g., Müller and Stein, 2014; Hoff et al., 2016) provide further evidence of
510 substantial climatic overprinting within biomarker profiles.

511 Resolving the relative contributions of climatic influence and diagenetic alteration on
512 downcore IP_{25} (and other biomarker) distributions is likely to remain a challenge from an
513 analytical perspective, however, not least because, on the basis of our new results described
514 here, the oxidation products of IP_{25} are unlikely to accumulate in sufficient amounts to enable
515 their quantification (or even detection), especially since IP_{25} content itself is often quite low in
516 Arctic marine sediments. On the other hand, the measurement of certain biomarker ratios such
517 as Bra/24-Me may prove useful for assessing such degradation processes, especially when
518 used alongside IP_{25} concentration profiles; however, the potential for changes in

519 environmental conditions to also influence such ratios should also be considered. Further, the
520 measurement of redox boundary layers in upper sections of sediment cores might also provide
521 additional insights into the nature of different degradation processes.

522 Finally, it is interesting to note that we were not able to detect any IP₂₅ oxidation
523 products in our sample of sea ice algae, which supports conclusions from previous studies that
524 it is largely resistant to abiotic alteration in the host matrix (Rontani et al., 2014) and also in
525 the water column soon after ice melt (Brown et al., 2016; Rontani et al., 2016).

526

527 **5. Conclusions**

528 This study represents the first attempt to evaluate, via oxidative product identification,
529 the possible fate of IP₂₅ in Arctic sediments. Laboratory-based autoxidation of the Arctic sea
530 ice diatom biomarker IP₂₅ results in the formation of a series of oxidation products that could
531 be characterised using high resolution GC–MS methods. Some of the same oxidation products
532 could also be identified in sediment material from the Canadian Arctic although their
533 accumulation was very low, likely due to further oxidation. The detection of bacterial
534 metabolites of IP₂₅ showed that this HBI alkene may also be affected by aerobic and/or
535 anaerobic degradation processes in sediments. We suggest that complementary evidence for
536 autoxidation and biodegradation processes may potentially be obtained from measurement of
537 certain phytoplankton sterol ratios, although these may also be influenced by changes to the
538 overlying climatic conditions.

539 Although degradation of IP₂₅ has, to date, not been considered in detail within IP₂₅-
540 based sea ice reconstructions, our initial overview of previous studies suggests that climatic
541 contributions to sedimentary IP₂₅ distributions likely exceed the impact of sedimentary
542 degradation, at least in the albeit still limited number of case studies thus far reported. On the
543 other hand, oxidative degradation may have a significant impact on IP₂₅ concentration in

544 some near-surface material, especially in cases where the oxic layer represents relatively long
545 time intervals. In any case, we suggest that such degradation processes should be considered
546 more carefully in future sea ice reconstructions based on IP₂₅.

547

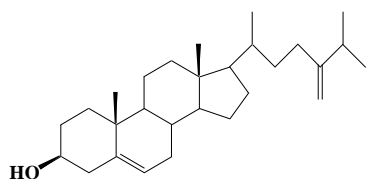
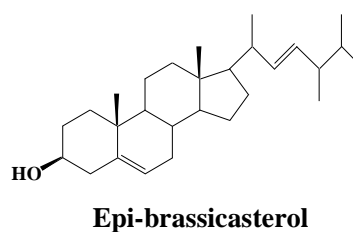
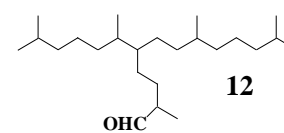
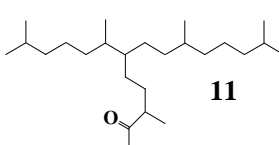
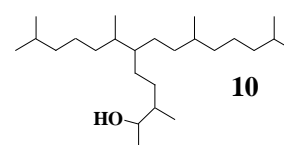
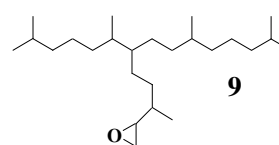
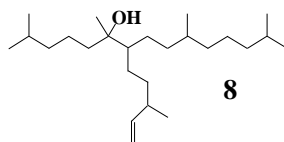
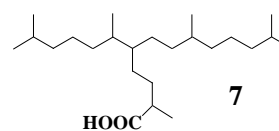
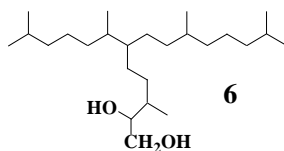
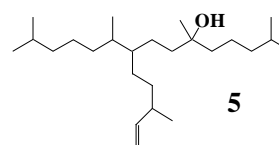
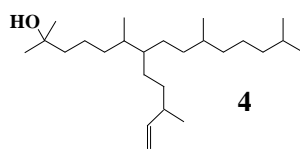
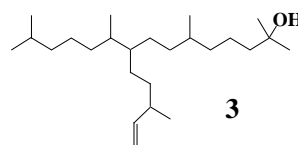
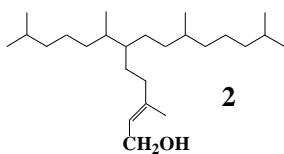
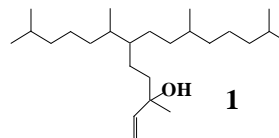
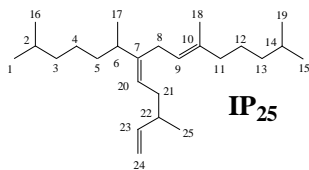
548 **Acknowledgments**

549 Financial support from the Centre National de la Recherche Scientifique (CNRS) and
550 the Aix-Marseille University is gratefully acknowledged. Thanks are due to the FEDER
551 OCEANOMED (N° 1166-39417) for the funding of the apparatus employed. We are grateful
552 to Lindsay Vare for providing us with the redox boundary information used in this study and
553 for carrying out some of the sediment extractions for IP₂₅ analysis. Patricia Cabedo-Sanz is
554 acknowledged for conducting calibration experiments that enabled us to subsequently
555 quantify IP₂₅ from archived GC–MS data. We also thank Thomas Brown for fruitful
556 discussions regarding the potential degradation of IP₂₅ in Arctic sediments. We are grateful to
557 Lindsay Vare, Guillaume Massé, André Rochon and the officers and crew of the CCGS
558 Amundsen for help with obtaining box core sediment material. Finally, we thank the
559 Associate Editor, Kirsten Fahl and an anonymous reviewer for their useful and constructive
560 comments.

561

562 *Associate Editor*–**Marcus Elvert**

APPENDIX



564 **References**

- 565 Alonso-García, M., Andrews, J.T., Belt, S.T., Cabedo-Sanz, P., Darby, D., Jaeger, J., 2013. A
566 comparison between multi-proxy and historical data (AD 1990-1840) of drift-ice
567 conditions on the East Greenland shelf (~66°N). *The Holocene* 23, 1672–1683.
- 568 Amiraux, R., Belt, S.T., Vaultier, F., Galindo, V., Gosselin, M., Bonin, P., Rontani, J.-F.,
569 2017. Monitoring of photooxidative and osmotic bacterial stresses in Arctic using
570 specific lipid tracers. *Marine Chemistry* (In press).
- 571 Andrews, J.T., Belt, S.T., Olafsdottir, S., Massé, G., Vare, L.L., 2009. Sea ice and climate
572 variability for NW Iceland/Denmark Strait over the last 2000 cal. yr BP. *The Holocene*
573 19, 775–784.
- 574 Belt, S.T., Müller, J., 2013. The Arctic sea ice biomarker IP₂₅: a review of current
575 understanding, recommendations for future research and applications in palaeo sea ice
576 reconstructions. *Quaternary Science Reviews* 79, 9–25.
- 577 Belt, S.T., Massé, G., Rowland, S.J., Poulin, M., Michel, C., LeBlanc, B., 2007. A novel
578 chemical fossil of palaeo sea ice: IP₂₅. *Organic Geochemistry* 38, 16–27.
- 579 Belt, S.T., Vare, L.L., Massé, G., Manners, H.R., Price, J.C., MacLachlan, S.E., Andrews, J.T.
580 and Schmidt, S., 2010. Striking similarities in temporal changes to seasonal sea ice
581 conditions across the central Canadian Arctic Archipelago over the last 7,000 years.
582 *Quaternary Science Reviews* 29, 3489–3504.
- 583 Belt, S.T., Brown, T.A., Navarro-Rodriguez, A., Cabedo-Sanz, P., Tonkin, A., Ingle, R.,
584 2012. A reproducible method for the extraction, identification and quantification of the
585 Arctic sea ice proxy IP₂₅ from marine sediments. *Analytical Methods* 4, 705–713.
- 586 Belt, S.T., Brown, T.A., Ringrose, A.E., Cabedo-Sanz, P., Mundy, C.J., Gosselin, M., Poulin,
587 M., 2013. Quantitative measurements of the sea ice diatom biomarker IP₂₅ and sterols

588 in Arctic sea ice and underlying sediments: Further considerations for palaeo sea ice
589 reconstruction. *Organic Geochemistry* 62, 33–45.

590 Belt, S.T., Cabedo-Sanz, P., Smik, L., Navarro-Rodriguez, A., Berben, S.M.P., Knies, J.,
591 Husum, K., 2015. Identification of paleo Arctic winter sea ice limits and the marginal
592 ice zone: optimised biomarker-based reconstructions of late Quaternary Arctic sea ice.
593 *Earth and Planetary Science Letters* 431, 127–139.

594 Berben, S.M.P., Husum, K., Cabedo-Sanz, P., Belt, S.T., 2014. Holocene sub-centennial
595 evolution of Atlantic Water inflow and sea ice distribution in the western Barents Sea.
596 *Climate of the Past* 10, 181–198.

597 Berben, S.M.P., Husum, K., Navarro-Rodriguez, A., Belt, S.T., Aagaard-Sørensen, S., 2017.
598 Semi-quantitative reconstruction of early to late Holocene spring and summer sea ice
599 conditions in the northern Barents Sea. *Journal of Quaternary Science* 32, 587–603.

600 Brown, T.A., 2011. Production and preservation of the Arctic sea ice diatom biomarker IP₂₅.
601 Ph.D. thesis. University of Plymouth, UK.

602 Brown, T.A., Belt, S.T., Tatarek, A., Mundy, C.J., 2014. Source identification of the Arctic
603 sea ice proxy IP₂₅. *Nature Communications* 5, 4197.

604 Brown, T.A., Belt, S.T., Gosselin, M., Levasseur, M., Poulin, M., Mundy, C.J., 2016.
605 Quantitative estimates of sinking sea ice particulate organic carbon based on the
606 biomarker IP₂₅. *Marine Ecology Progress Series* 546, 17–29.

607 Cabedo-Sanz, P., Belt, S.T., 2016. Seasonal sea ice variability in eastern Fram Strait over the
608 last 2,000 years. *Arktos* 2, 22.

609 Cabedo-Sanz, P., Belt, S.T., Knies, J.K., Husum, K., 2013. Identification of contrasting
610 seasonal sea ice conditions during the Younger Dryas. *Quaternary Science Reviews*
611 79, 74–86.

- 612 Cantwell, S.G., Lau, E.P., Watt, D.S., Fall, R.R., 1978. Biodegradation of acyclic isoprenoids
613 by *Pseudomonas* species. *Journal of Bacteriology* 135, 324–333.
- 614 Chiang, Y.-R., Ismael, W., Müller, M., Fuchs, G., 2007. Initial steps in the anoxic metabolism
615 of cholesterol by the denitrifying *Sterolibacterium denitrificans*. *The Journal of*
616 *Biological Chemistry* 282, 13240–13249.
- 617 Christodoulou, S., Marty, J.-C., Miquel, J.-C., Volkman, J.K., Rontani, J.-F., 2009. Use of
618 lipids and their degradation products as biomarkers for carbon cycling in the
619 northwestern Mediterranean Sea. *Marine Chemistry* 113, 25–40.
- 620 Cormier, M.-A., Rochon, A., de Vernal, A., Gélinas, Y., 2016. Multi-proxy study of primary
621 production and paleoceanographical conditions in northern Baffin Bay during the last
622 centuries. *Marine Micropaleontology* 127, 1–10.
- 623 Darby, D.A., Polyak, L., Bauch, H.A., 2006. Past glacial and interglacial conditions in the
624 Arctic Ocean and marginal seas – a review. *Progress in Oceanography* 71, 129–144.
- 625 Detlef, H., Belt, S.T., Sosdian, S.M., Smik, L., Lear, C.H., Hall, I.R., Cabedo-Sanz, P,
626 Husum, K., Kender, S., 2017. Changes in sea ice dynamics in the eastern Bering Sea
627 during the Mid-Pleistocene climate transition. *Nature Communications* (in press).
- 628 Fahl, K., Stein, R., 2012. Modern seasonal variability and deglacial/Holocene change of
629 central Arctic Ocean sea-ice cover: new insights from biomarker proxy records. *Earth*
630 *and Planetary Science Letters* 351-352, 123–133.
- 631 Fenchel, T., King, G.M., Blackburn, T.H., 1998. *Bacterial Biogeochemistry: The*
632 *Ecophysiology of Mineral Cycling*. Academic Press, NY.
- 633 Fuchs, C., Spiteller, G., 2014. Iron release from the active site of lipooxygenase. *Zeitschrift für*
634 *Naturforschung C* 55, 643–648.
- 635 Galeron, M.-A., Radakovitch, O., Charriere, B., Vaultier, F., Volkman, J.K., Bianchi, T.S.,
636 Ward, N.T., Medeiros, P., Sawakuchi, H., Tank, S., Kerhervé, P., Rontani J-F., 2018.

- 637 Lipoxygenase-induced autoxidative degradation of terrestrial particulate organic
638 matter in estuaries: a widespread process enhanced at high and low latitudes. *Organic*
639 *Geochemistry* 115, 78-92.
- 640 Grossi, V., Blokker, P., Sinninghe Damsté, J.S., 2001. Anaerobic biodegradation of lipids of
641 the marine microalga *Nannochloropsis salina*. *Organic Geochemistry* 32, 795–808.
- 642 Hartnett, H.E., Keil, R.G., Hedges, J.I., Devol, A.H., 1998. Influence of oxygen exposure time
643 on organic carbon preservation in continental margin sediments. *Nature* 391, 572–574.
- 644 Henrich, R., 1991. Cycles, rhythms, and events on high input and low input glaciated
645 continental margins. In: Einsele, G., Ricken, W., Seilacher, A. (Eds), *Cycles and*
646 *Events in Stratigraphy*. Springer, Berlin Heidelberg, pp. 751–772.
- 647 Hoff, U., Rasmussen, T.L., Stein, R., Ezat, M.M., Fahl, K., 2016. Sea ice and millennial-scale
648 climate variability in the Nordic Seas 90 kyr ago to present. *Nature Communications*
649 7, 12247.
- 650 Hörner, T., Stein, R., Fahl, K., Birgel, D., 2016. Post-glacial variability of sea ice cover, river
651 run-off and biological production in the western Laptev Sea (Arctic Ocean) - A high
652 resolution biomarker study. *Quaternary Science Reviews* 143, 133–149.
- 653 Hörner, T., Stein, R., Fahl, K., 2017. Evidence for Holocene centennial variability in sea ice
654 cover based on IP₂₅ biomarker reconstruction in the southern Kara Sea (Arctic Ocean).
655 *Geo-Marine Letters* doi: 10.1007/s00367-00017-00501-y.
- 656 Hurst, J.R., Wilson, S.L., Schuster, G.B., 1985. The ene reaction of singlet oxygen: kinetic
657 and product evidence in support of a perepoxy intermediate. *Tetrahedron* 41, 2191–
658 2197.
- 659 Jennings, A.E., Andrews, J.T., Ó Cofaigh, C., St. Onge, G., Sheldon, C., Belt, S.T., Cabedo-
660 Sanz, P., Hillaire-Marcel, C., 2017. Ocean forcing of Ice Sheet retreat in central west
661 Greenland from LGM to the early Holocene. *Earth and Planetary Science Letters* 472,

- 662 1–13.
- 663 Knies, J., Cabedo-Sanz, P., Belt, S.T., Baranwal, S., Fietz, S., Rosell-Melé, A., 2014. The
664 emergence of modern sea ice cover in the Arctic Ocean. *Nature Communications* 5,
665 5608.
- 666 Kölling, H.M., Stein, R., Fahl, K., Perner, P., Moros, M., 2017. Short-term variability in late
667 Holocene sea ice cover on the East Greenland Shelf and its driving mechanisms.
668 *Palaeogeography Palaeoclimatology Palaeoecology* doi.
669 10.1016/j.palaeo.2017.06.024.
- 670 Köseoğlu, D., Belt, S.T., Smik, L., Yao, H., Panieri, G., Knies, J., 2017. Complementary
671 biomarker-based methods for characterising Arctic sea ice conditions: A case study
672 comparison between multivariate analysis and the PIP₂₅ index. *Geochimica et*
673 *Cosmochimica Acta* 222, 406–420.
- 674 Kristensen, E., 2000. Organic matter diagenesis at the oxic/anoxic interface in coastal marine
675 sediments, with emphasis on the role of burrowing. *Hydrobiologia* 426, 1–24.
- 676 McCloskey, J.A., McClelland, M.J., 1965. Mass spectra of O-isopropylidene derivatives of
677 unsaturated fatty esters. *Journal of the American Chemical Society* 87, 5090–5093.
- 678 Maiti, K., Carroll, J., Benitez-Nelson, C.R., 2010. Sedimentation and particle dynamics in the
679 seasonal ice zone of the Barents Sea. *Journal of Marine Systems* 79, 185–198.
- 680 Massé, G., Rowland, S.J., Sicre, M.-A., Jacob, J., Jansen, E., Belt, S.T., 2008. Abrupt climate
681 changes for Iceland during the last millennium: Evidence from high resolution sea ice
682 reconstructions. *Earth and Planetary Science Letters* 269, 565–569.
- 683 Méheust, M., Stein R., Fahl, K., Max, L., Riethdorf, J.R., 2015. High-resolution IP₂₅-based
684 reconstruction of sea-ice variability in the western North Pacific and Bering Sea
685 during the past 18,000 years. *Geo-Marine Letters* 36, 101–111.

- 686 Morgan, P., Watkinson, R.J., 1994. Biodegradation of components of petroleum. In: Ratledge,
687 C. (Ed.), *Biochemistry of Microbial Degradation*. Kluwer Academic Publishers,
688 Dordrecht, pp. 1–25.
- 689 Mudie, P.J., Rochon, A., Prins, M.A., Soenarjo, D., Troelstra, S.R., Levac, E., Scott, D.B.,
690 Roncaglia, L., Kuijpers, A., 2006. Late Pleistocene-Holocene marine geology of Nares
691 Strait region: palaeoceanography from foraminifera and dinoflagellate cysts,
692 sedimentology and stable isotopes. *Polarforschung* 74, 169–183.
- 693 Müller, J., Stein, R., 2014. High-resolution record of late glacial sea ice changes in Fram
694 Strait corroborates ice-ocean interactions during abrupt climate shifts. *Earth and
695 Planetary Science Letters* 403, 446–455.
- 696 Müller, J., Massé, G., Stein, R., Belt, S.T., 2009. Variability of sea-ice conditions in the Fram
697 Strait over the past 30,000 years. *Nature Geoscience* 2, 772–776.
- 698 Müller, J., Wagner, A., Fahl, K., Stein, R., Prange, M., Lohmann, G., 2011. Towards
699 quantitative sea ice reconstructions in the northern North Atlantic: A combined
700 biomarker and numerical modelling approach. *Earth and Planetary Science Letters*
701 306, 137–148.
- 702 Müller, J., Werner, K., Stein, R., Fahl, K., Moros, M., Jansen, E., 2012. Holocene cooling
703 culminates in sea ice oscillations in Fram Strait. *Quaternary Science Reviews* 47, 1–
704 14.
- 705 Navarro-Rodriguez, A., Belt, S.T., Brown, T.A., Knies, J., 2013. Mapping recent sea ice
706 conditions in the Barents Sea using the proxy biomarker IP₂₅: implications for palaeo
707 sea ice reconstructions. *Quaternary Science Reviews* 79, 26–39.
- 708 Philipp, B., 2011. Bacterial degradation of bile acids. *Applied Microbiology and
709 Biotechnology* 89, 903–915.

- 710 Polyak, L., Belt, S.T., Cabedo-Sanz, P., Yamamoto, M., Park, Y.-H., 2016. Holocene sea-ice
711 conditions and circulation at the Chukchi-Alaskan margin, Arctic Ocean, inferred
712 from biomarker proxies. *The Holocene* 26, 1810–1821.
- 713 Ratledge, C., 1994. Biodegradation of oils, fats and fatty acids. In: Ratledge, C. (Ed.),
714 *Biochemistry of Microbial Degradation*. Kluwer Academic Publishers, Dordrecht, pp.
715 89–142.
- 716 Resch, V., Hanefeld, U., 2015. The selective addition of water. *Catalysis Science and*
717 *Technology* 5, 1385–1399.
- 718 Ribeiro, S., Sejr, M.K., Limoges, A., Heikkilä, M., Andersen, T.J., Tallberg, P., Weckström,
719 K., Husum, K., Forwick, M., Dalsgaard, T., Massé, G., Seidenkrantz, M.-S., Rysgaard,
720 S., 2017. Sea ice and primary production proxies in surface sediments from a High
721 Arctic Greenland fjord: Spatial distribution and implications for palaeoenvironmental
722 studies. *Ambio* 46(Suppl. 1), S106–S118.
- 723 Robson, J.N., 1987. Synthetic and biodegradation studies of some sedimentary isoprenoid
724 hydrocarbons. PhD thesis, Plymouth Polytechnic, Plymouth.
- 725 Robson, J.N., Rowland, S.J., 1988. Biodegradation of highly branched isoprenoid
726 hydrocarbons: a possible explanation of sedimentary abundance. *Organic*
727 *Geochemistry* 13, 691–695.
- 728 Rontani, J.-F., 2012. Photo-and free radical-mediated oxidation of lipid components during
729 the senescence of phototrophic organisms. In: Nagata, T. (Ed.), *Senescence*. Intech,
730 Rijeka, pp. 3–31.
- 731 Rontani, J.-F., Volkman, J.K., 2003. Phytol degradation products as biogeochemical tracers in
732 aquatic environments. *Organic Geochemistry* 34, 1–35.

- 733 Rontani, J.-F., Bonin, P., Volkman, J.K., 1999. Biodegradation of free phytol by bacterial
734 communities isolated from marine sediments under aerobic and denitrifying
735 conditions. *Applied and Environmental Microbiology* 65, 5484–5492.
- 736 Rontani, J.-F., Zabeti, N., Wakeham, S.G., 2009. The fate of marine lipids: biotic vs. abiotic
737 degradation of particulate sterols and alkenones in the Northwestern Mediterranean
738 Sea. *Marine Chemistry* 113, 9-18.
- 739 Rontani, J.-F., Belt, S.T., Vaultier, F., Brown, T.A., 2011. Visible light induced photo-
740 oxidation of highly branched isoprenoid (HBI) alkenes: Significant dependence on the
741 number and nature of double bonds. *Organic Geochemistry* 42, 812–822.
- 742 Rontani, J.-F., Charrière, B., Forest, A., Heussner, S., Vaultier, F., Petit, M., Delsaut, N.,
743 Fortier, L., Sempéré, R., 2012. Intense photooxidative degradation of planktonic and
744 bacterial lipids in sinking particles collected with sediment traps across the Canadian
745 Beaufort Shelf (Arctic Ocean). *Biogeosciences* 9, 4787–4802.
- 746 Rontani, J.-F., Bonin, P., Vaultier, F., Guasco, S., Volkman, J.K., 2013. Anaerobic bacterial
747 degradation of pristenes and phytene in marine sediments does not lead to pristane
748 and phytane. *Organic Geochemistry* 58, 43–55.
- 749 Rontani, J.-F., Belt, S.T., Vaultier, F., Brown, T.A., Massé, G., 2014. Autoxidation and
750 photooxidation of highly branched isoprenoid (HBI) alkenes: a combined kinetic and
751 mechanistic study. *Lipids* 49, 481–494.
- 752 Rontani, J.-F., Belt, S.T., Brown, T.A., Amiriaux, R., Gosselin, M., Vaultier, F., Mundy, C.J.,
753 2016. Monitoring abiotic degradation in sinking versus suspended Arctic sea ice algae
754 during a spring ice melt waters using specific lipid oxidation tracers. *Organic*
755 *Geochemistry* 98, 82–97.
- 756 Rontani, J.-F., Galeron, M.-A., Amiriaux, R., Artigue, L., Belt, S.T., 2017. Identification of di-
757 and triterpenoid lipid tracers confirms the significant role of autoxidation in the

- 758 degradation of terrestrial vascular plant material in the Canadian Arctic. *Organic*
759 *Geochemistry* 108, 43–50.
- 760 Rostoniec, K.Z., Wilbrink, M.H., Capyk, J.K., Mohn, W.W., Ostendorf, M., van der Geize,
761 R., Dijkhuisen, L., Eltis, L.D., 2009. Cytochrome P450 125 (CYP125) catalyses C26-
762 hydroxylation to initiate sterol side-chain degradation in *Rhodococcus jostii* RHA.
763 *Molecular Microbiology* 74, 1031–1043.
- 764 Schaich, K.M., 2005. Lipid Oxidation: Theoretical Aspects. In: Shahidi, F. (Ed.), *Bailey’s*
765 *Industrial Oil and Fat Products*. John Wiley & Sons, Chichester, pp. 269–355.
- 766 Seki, H., Ohyama, K., Sawai, S., Mizutani, M., Ohnishi, T., Sudo, H., Akashi, T., Aoki, T.,
767 Saito, K., Muranaka, T., 2008. Licorice β -amyrin 11-oxidase, a cytochrome P450 with
768 a key role in the biosynthesis of the triterpene sweetener glycyrrhizin. *Proceedings of*
769 *the National Academy of Science of the United States of America* 105, 14204–14209.
- 770 Sojo, M., Bru, R., Lopez-Molina, D., Garcia-Carmona, F., Arguelles, J.C., 1997. Cell-linked
771 and extracellular cholesterol oxidase activities from *Rhodococcus erythropolis*.
772 *Isolation and physiological characterization*. *Applied and Environmental*
773 *Biotechnology* 47, 583–589.
- 774 Soltani, M., Metzger, P., Largeau, C., 2004. Effects of hydrocarbon structure on fatty acid,
775 fatty alcohols and β -hydroxy acid composition in the hydrocarbon-degrading
776 bacterium *Marinobacter hydrocarbonoclasticus*. *Lipids* 39, 491–505.
- 777 Stein, R., Fahl, K., 2000. Holocene accumulation of organic carbon at the Laptev Sea
778 continental margin (Arctic Ocean): sources, pathways, and sinks. *Geo-Marine Letters*
779 20, 27–36.
- 780 Stein, R., Fahl, K., 2013. Biomarker proxy IP₂₅ shows potential for studying entire Quaternary
781 Arctic sea-ice history. *Organic Geochemistry* 55, 98–102.
- 782 Stein, R., Nam, S.I., Schubert, C., Vogt, C., Fütterer, D., Heinemeier, J., 1994a. The last

- 783 deglaciation event in the eastern Central Arctic Ocean. *Science* 264, 692–696.
- 784 Stein, R., Schubert, C., Vogt, C., Fütterer, D., 1994b. Stable isotope stratigraphy, sedimentation
785 rates, and salinity changes in the Latest Pleistocene to Holocene eastern central Arctic
786 Ocean. *Marine Geology* 119, 333–355.
- 787 Stein, R., Fahl, K., Schade, I., Manerung, A., Wassmuth, S., Niessen, F., Nam, S., 2017.
788 Holocene variability in sea ice cover, primary production, and Pacific-Water inflow
789 and climate change in the Chukchi and East Siberian Seas (Arctic Ocean). *Journal of*
790 *Quaternary Science* 32, 362–379.
- 791 Stoyanova, V., Shanahan, T.M., Hughen, K.A., de Vernal, A., 2013. Insights into circum-
792 Arctic sea ice variability from molecular geochemistry. *Quaternary Science Reviews*
793 79, 63–73.
- 794 Vare, L.L., Massé, G., Belt, S.T., 2010. A biomarker-based reconstruction of sea ice
795 conditions for the Barents Sea in recent centuries. *The Holocene* 40, 637–643.
- 796 Vare, L.L., Massé, G., Gregory, T.R., Smart, C.W., Belt, S.T., 2009. Sea ice variations in the
797 central Canadian Arctic Archipelago during the Holocene. *Quaternary Science*
798 *Reviews* 28, 1354–1366.
- 799 Weckström, K., Massé, G., Collins, L.G., Hanhijärvi, S., Bouloubassi, I., Sicre, M.-A.,
800 Seidenkrantz, M.-S., Schmidt, S., Andersen, T.J., Andersen, M.L., Hill, B., Kuijpers,
801 A., 2013. Evaluation of the sea ice proxy IP₂₅ against observational and diatom proxy
802 data in the SW Labrador Sea. *Quaternary Science Reviews* 79, 53–62.
- 803 Xiao, X., Stein, R., Fahl, K., 2013. Biomarker distributions in surface sediments from the
804 Kara and Laptev Seas (Arctic Ocean): Indicators for organic-carbon sources and sea
805 ice coverage. *Quaternary Science Reviews* 79, 40–52.

806 Xiao, X., Fahl, K., Müller, J., Stein, R., 2015. Sea-ice distribution in the modern Arctic
807 Ocean: Biomarker records from trans-Arctic Ocean surface sediments. *Geochimica et*
808 *Cosmochimica Acta* 155, 16–29.

809

810

811

812

813

814

815 **Figure captions**

816

817 **Fig. 1.** Map showing the sampling locations.

818

819 **Fig. 2.** TOFMS mass spectra of HBI alcohol trimethylsilyl derivatives of: (A) 3,9,15-
820 trimethyl-6-(1,5-dimethylhexyl)-tetradec-1-en-3-ol (**1**), (B) 2,6,10,14-tetramethyl-7-(3-
821 methylpent-4-enyl)-pentadecan-2-ol (**4**) and (C) 2,6,10,14-tetramethyl-9-(3-methylpent-4-
822 enyl)-pentadecan-6-ol (**5**).

823

824 **Fig. 3.** Downcore plots of IP₂₅ concentration and the epi-brassicasterol/24-
825 methylenecholesterol (Bra/24-Me) ratio for the three stations investigated. (The dashed lines
826 represent the redox boundaries).

827

828 **Fig. 4.** Partial ion chromatograms (m/z 131.0885, 143.0883, 201.1670 and 423.4015 (M –
829 CH₃)) showing the distribution of IP₂₅ oxidation products obtained after incubation in the
830 presence of *tert*-butyl hydroperoxide and di-*tert*-butyl nitroxide at 65 °C under darkness (A)
831 and present in the 2–3 cm layer of the core sediment from the station 4 (B). The peak labelled
832 * represents a compound tentatively identified as 2,6,10,14-tetramethyl-7-(3-methylpent-4-
833 yl)-pentadecan-6-ol (**8**) trimethylsilyl derivative.

834

835 **Fig. 5.** Partial ion chromatograms (m/z 425.4174 and 513.4520 (M – CH₃)) showing the
836 diastereoisomers of 3,9,15-trimethyl-6-(1,5-dimethylhexyl)-tetradecan-1,2-diol trimethylsilyl
837 ether obtained after oxidation of IP₂₅ with OsO₄ (A) and present in the 2–3 cm (B) and 4–5
838 cm layers of the core from Barrow Strait (STN 4) (C) and the 2–3 cm layer of the core from
839 the western Amundsen Gulf (STN 408) (D).

840

841 **Fig. 6.** Partial ion chromatograms (m/z 146.0755 and 425.3802 ($M - CH_3$)) showing 2,8,12-
842 trimethyl-5-(1,5-dimethylhexyl)-tridecanoic acid trimethylsilyl derivative obtained after OsO_4
843 oxidation of IP_{25} (A) and present in the 2–3 cm layer of the core sediment from Barrow Strait
844 (STN 4) (B) and Viscount Melville Sound (STN 308) (C).

845

846 **Fig. 7.** TOFMS mass spectra of HBI trimethylsilyl derivatives of: (A) 3,9,15-trimethyl-6-(1,5-
847 dimethylhexyl)-tetradecan-1,2-diol (**6**) and (B) 2,8,12-trimethyl-5-(1,5-dimethylhexyl)-
848 tridecanoic acid (**7**).

849

850 **Fig. 8.** Proposed mechanisms for the autoxidative degradation of IP_{25} .

851

852 **Fig. 9.** Proposed mechanisms for the aerobic bacterial degradation of the alkyl side-chain of
853 epi-brassicasterol and 24-methylenecholesterol.

854

855 **Fig. 10.** Proposed mechanisms for the aerobic and anaerobic bacterial degradation of IP_{25} .

856

857

publication version. Readers are recommended to use the published version for accuracy and citation.”

Figure 1

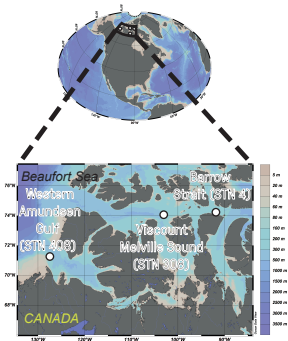
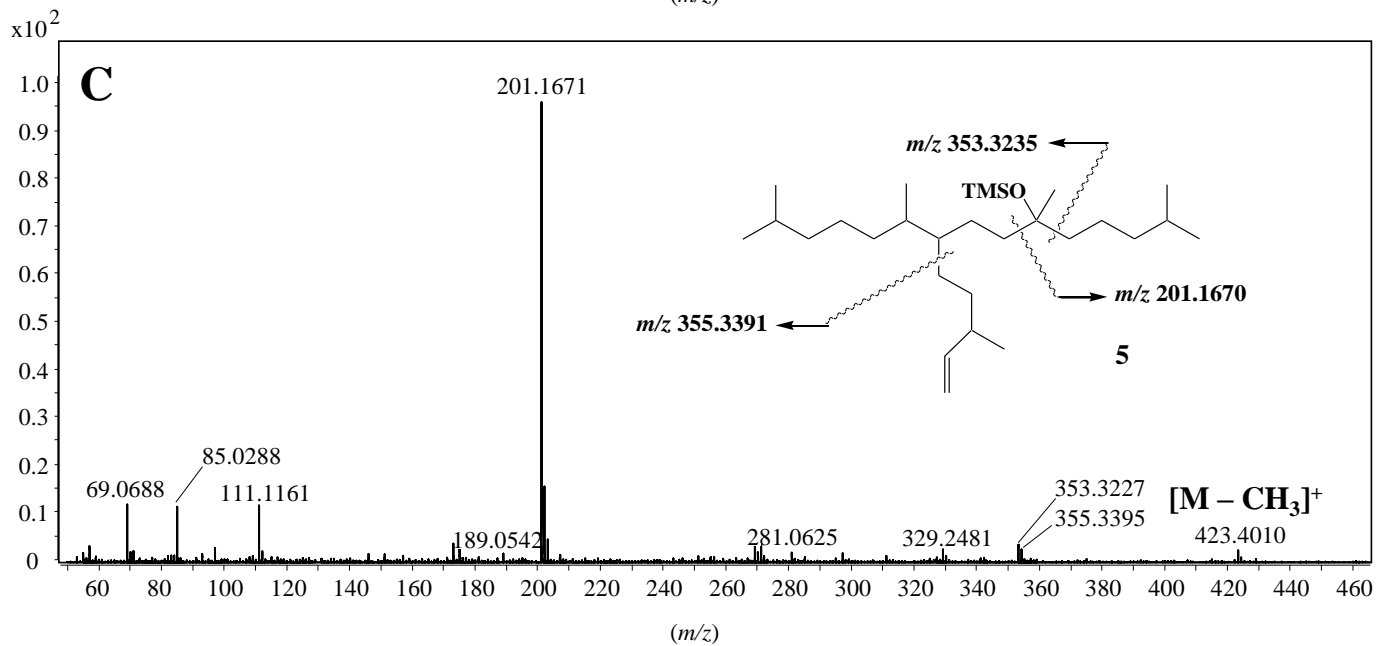
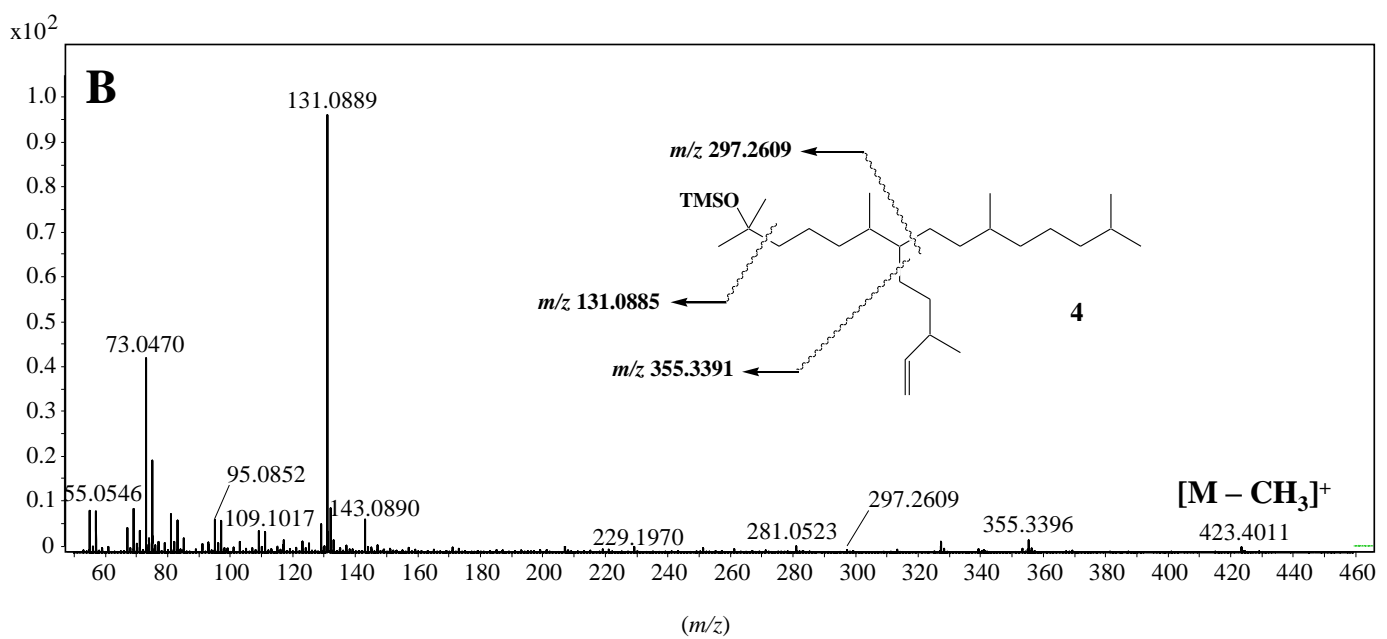
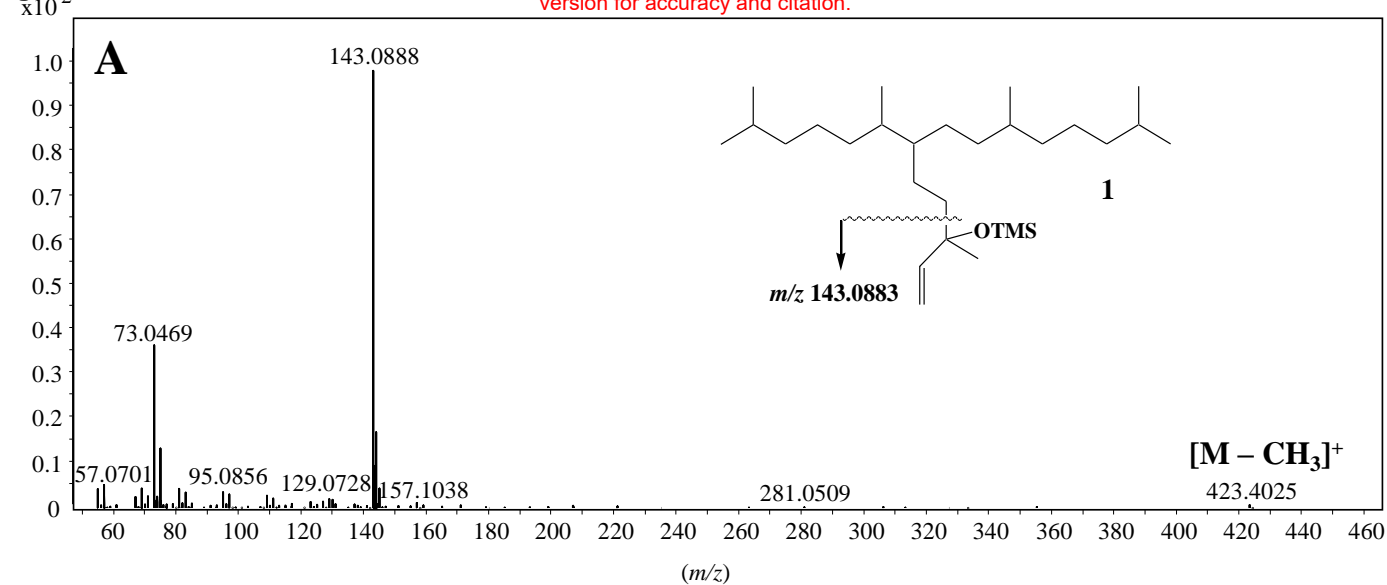
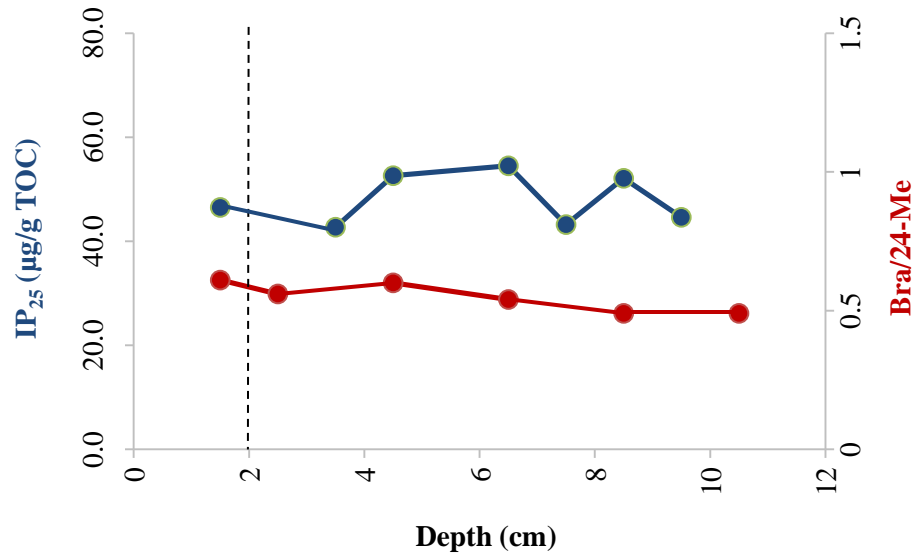


Figure 2

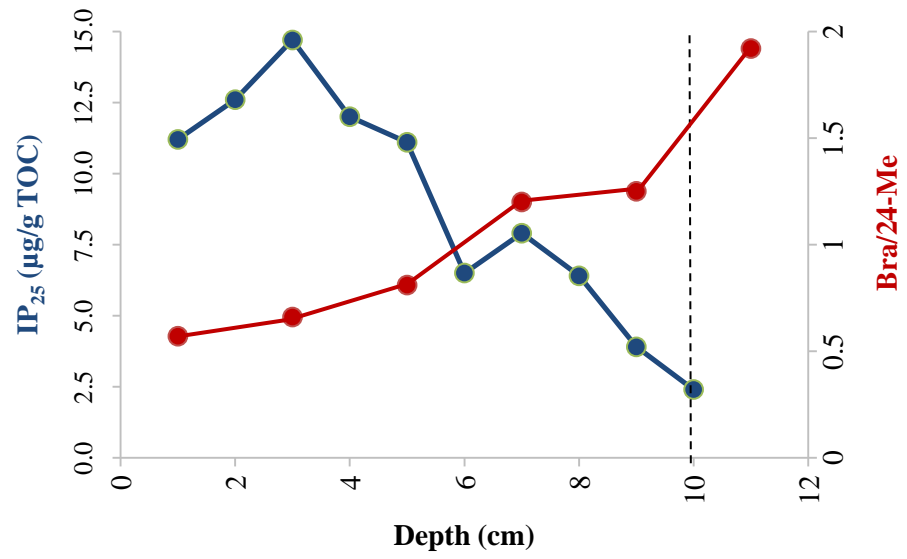
"Disclaimer: This is a pre-publication version. Readers are recommended to consult the full published version for accuracy and citation."



**Barrow Strait
(STN 4)**



**Viscount Melville Sound
(STN 308)**



**Western Amundsen Gulf
(STN 408)**

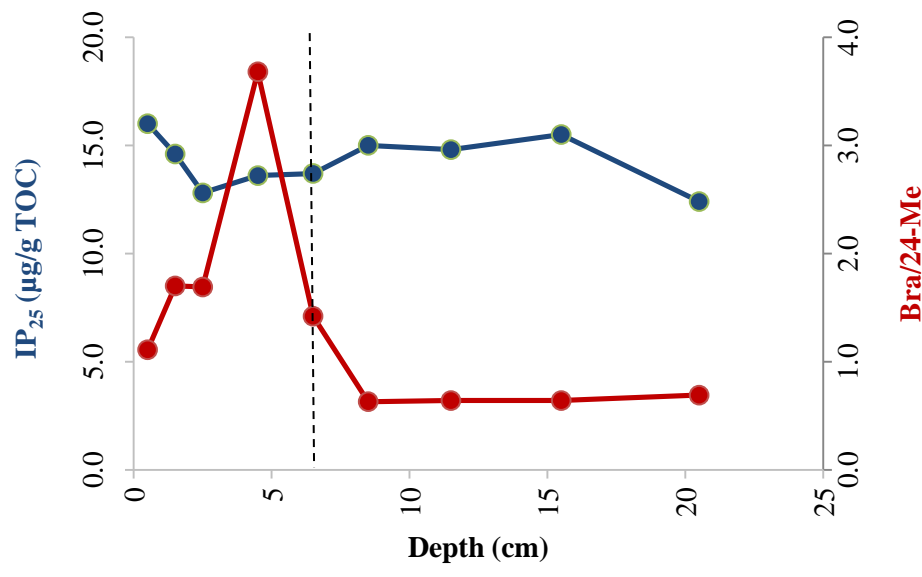


Figure 5

"Disclaimer: This is a pre-publication version. Readers are recommended to consult the full published version for accuracy and citation."

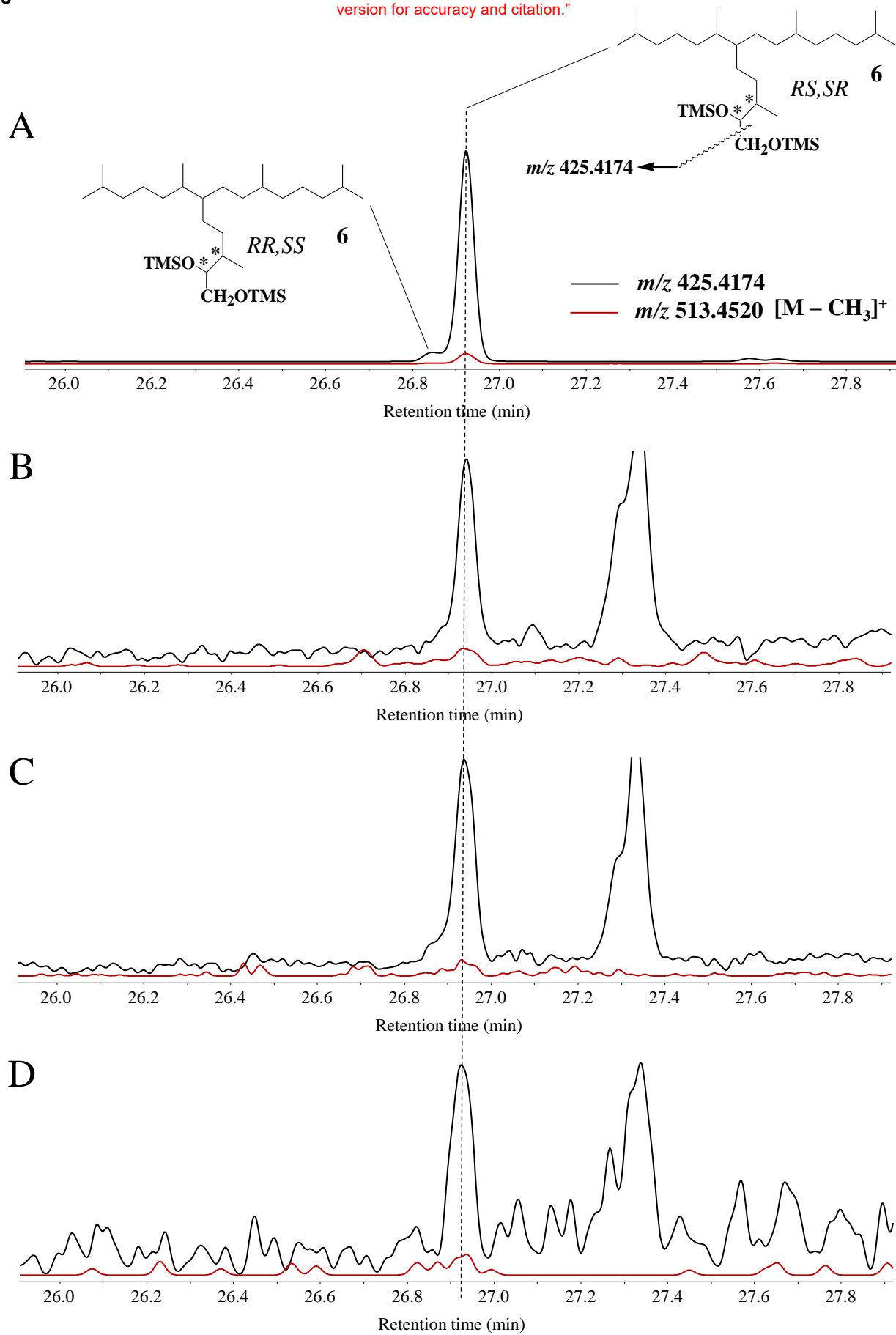
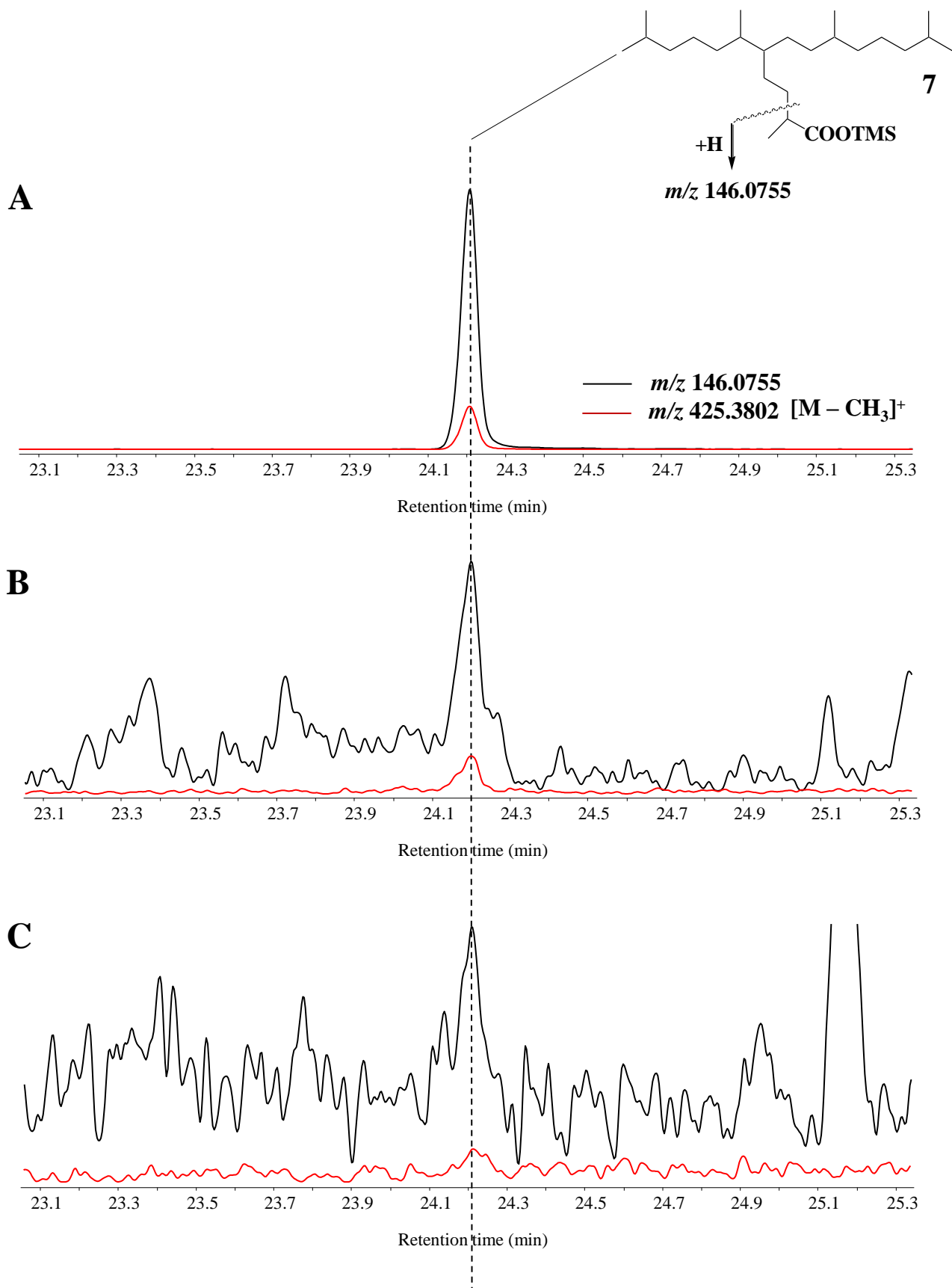


Figure 6

" Disclaimer: This is a pre-publication version. Readers are recommended to consult the full published version for accuracy and citation."



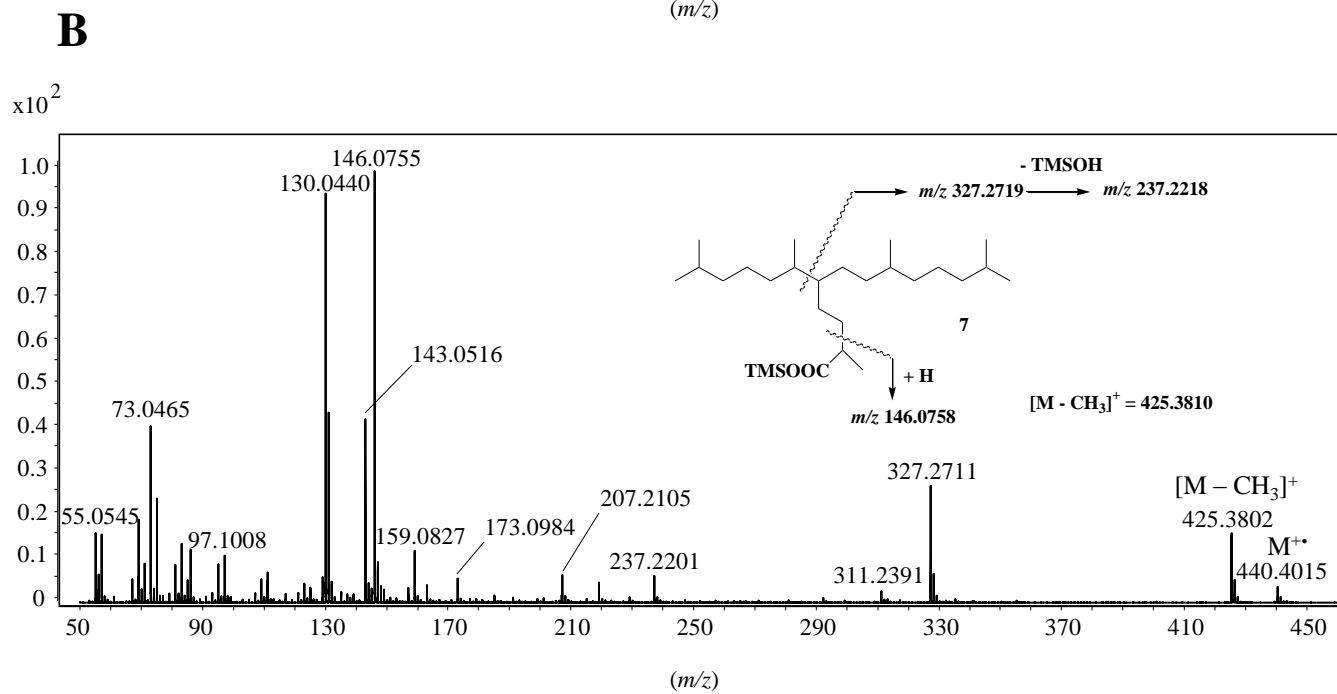
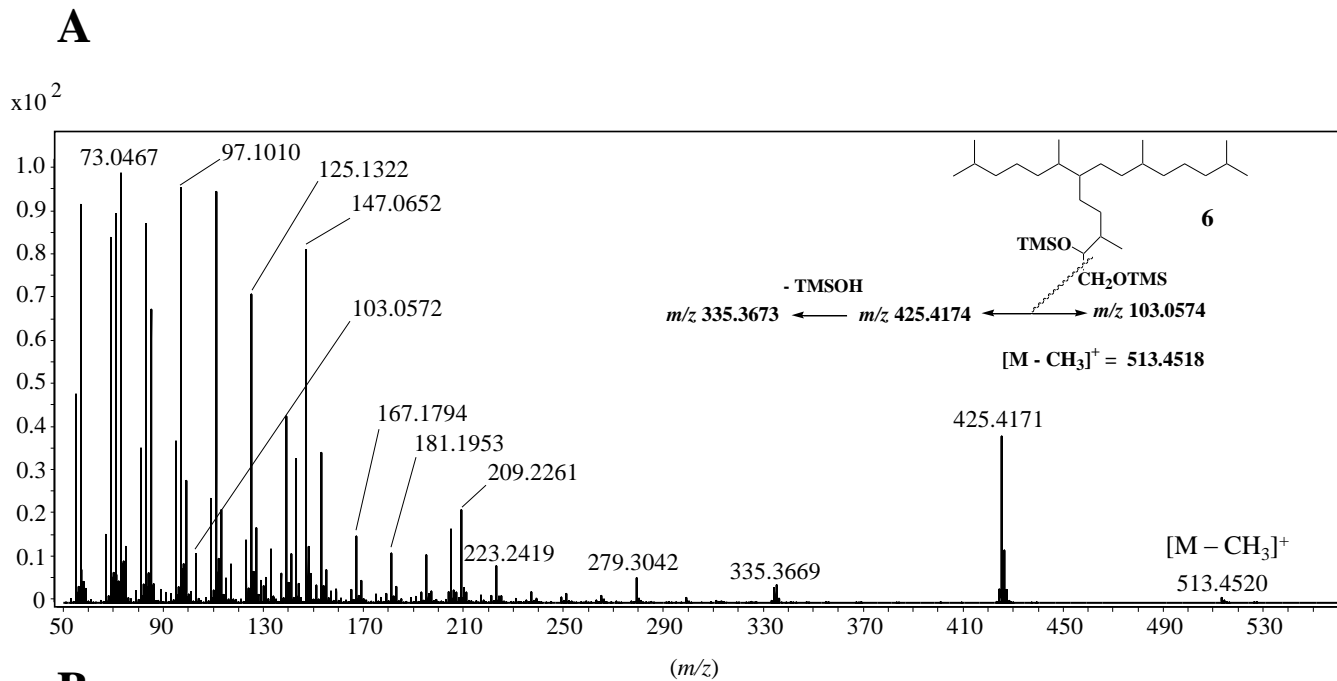


Figure 8

"Disclaimer: This is a pre-publication version. Readers are recommended to consult the full published version for accuracy and citation."

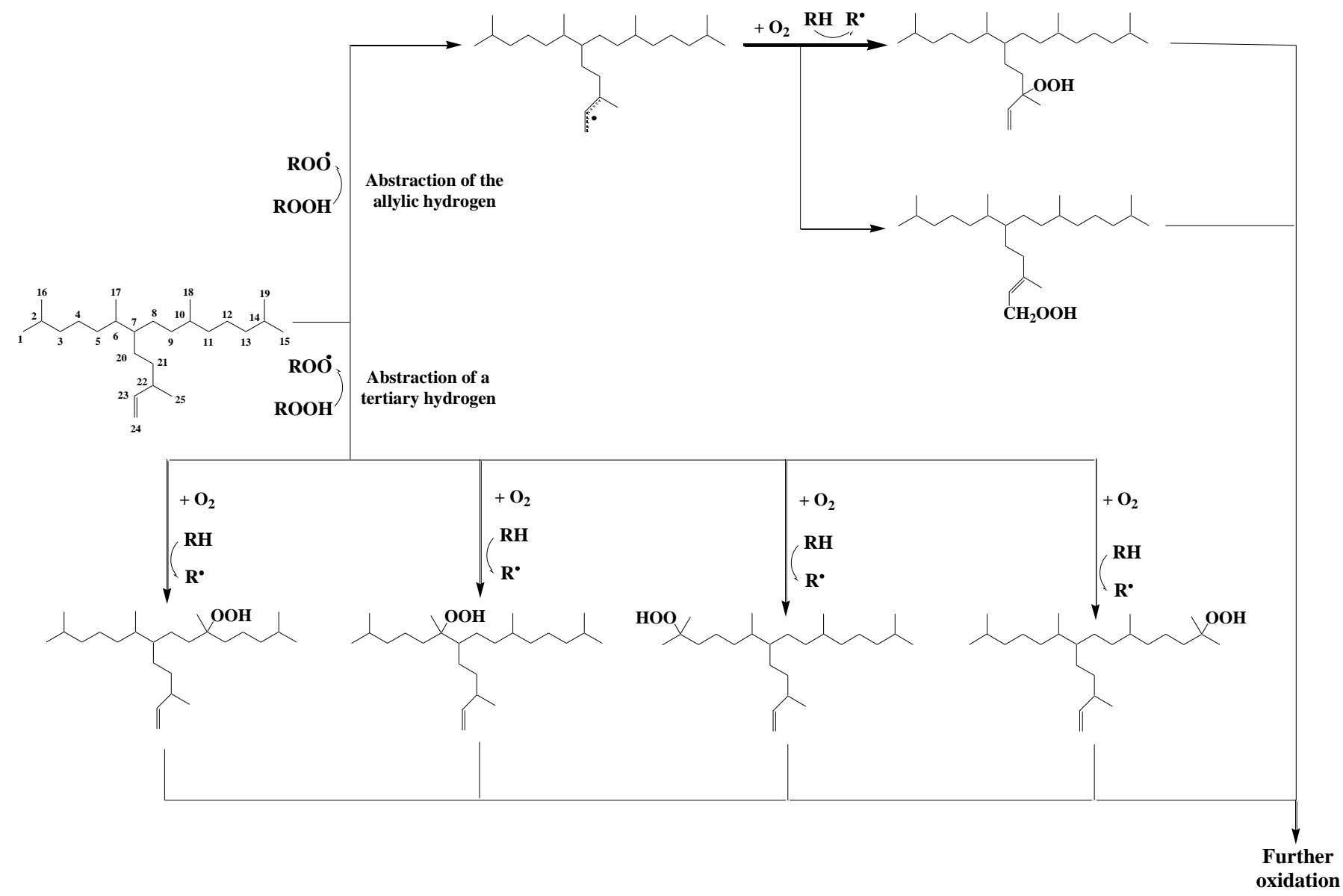
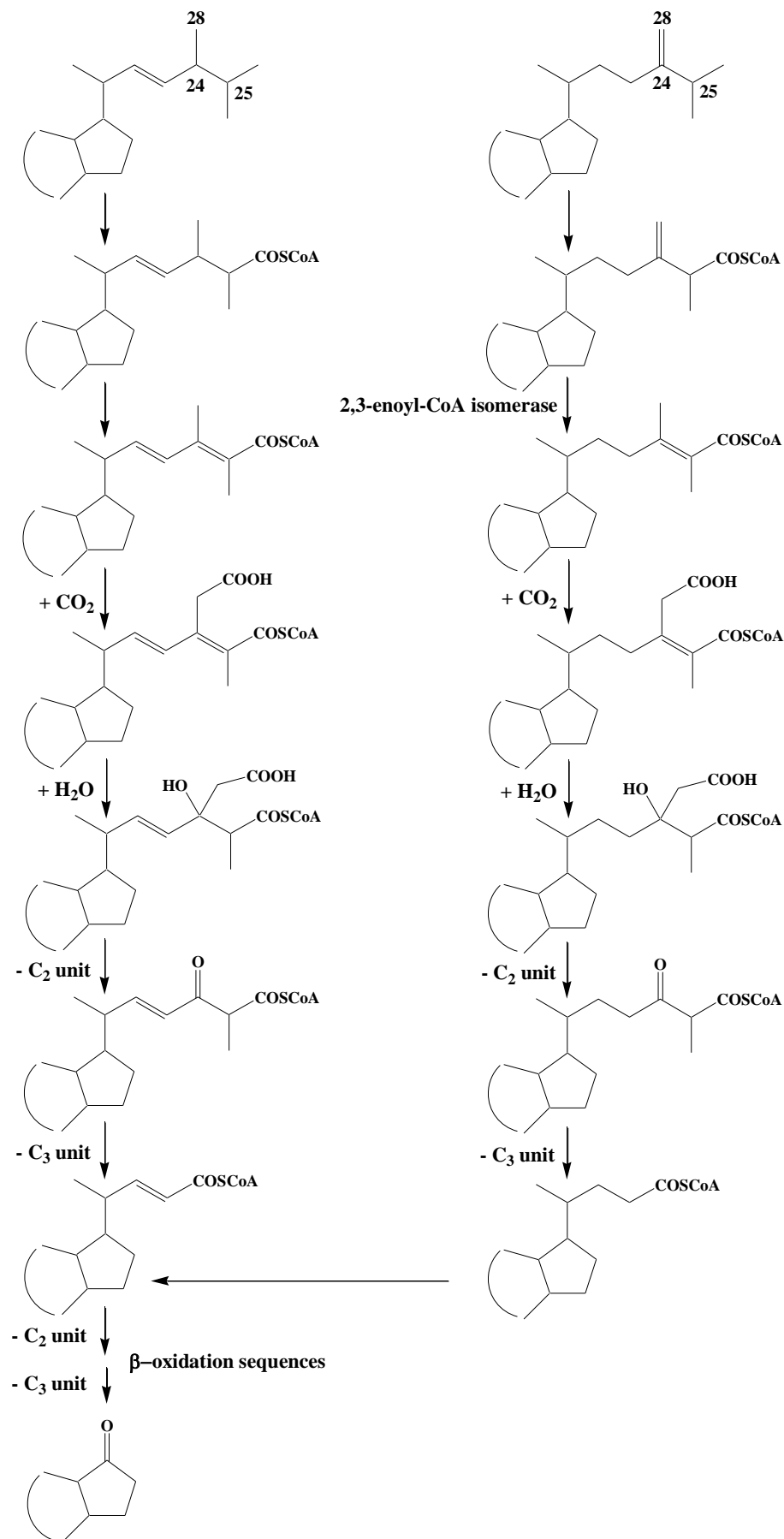


Figure 9

“Disclaimer: This is a pre-publication version. Readers are recommended to consult the full published version for accuracy and citation.”



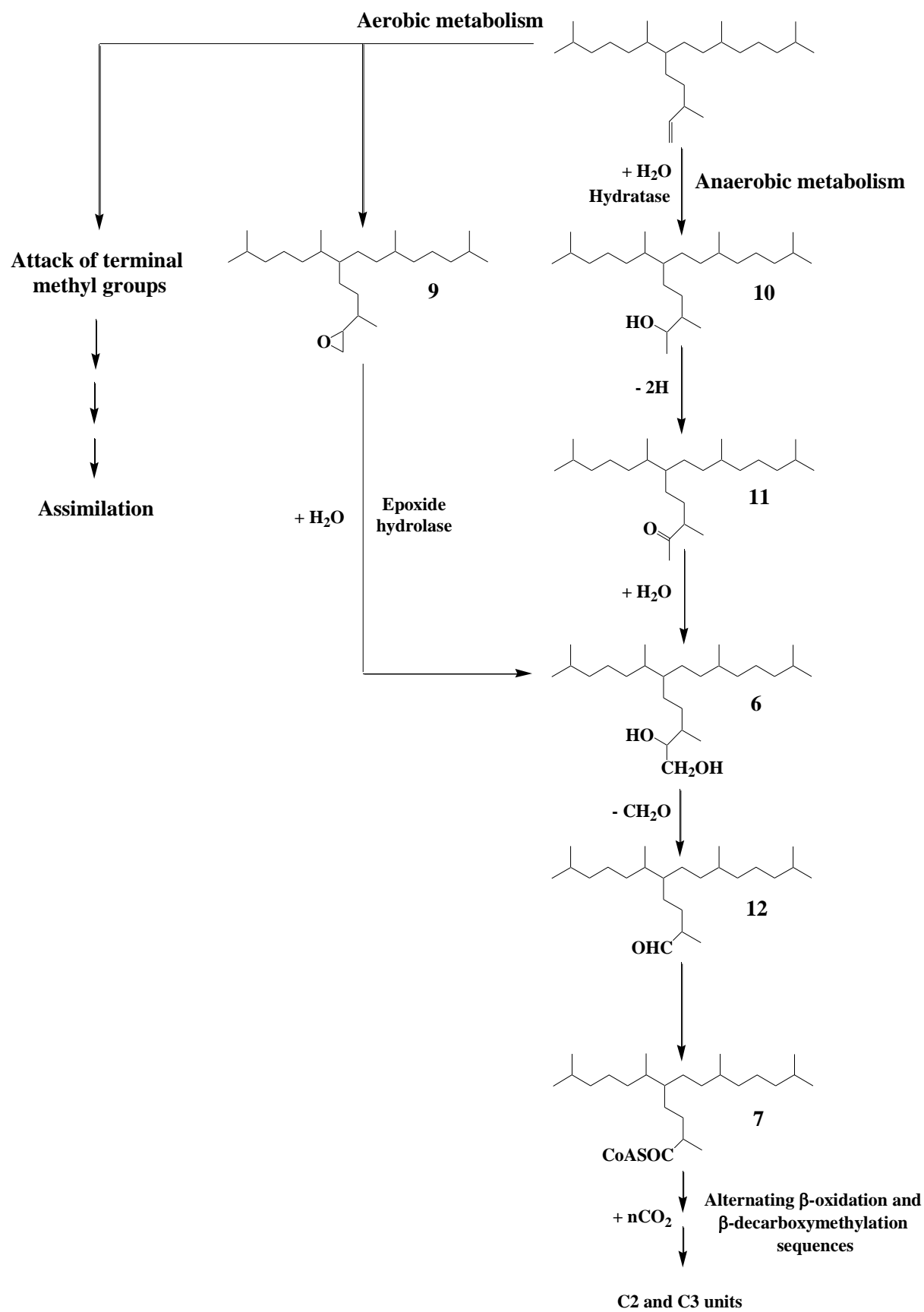


Table 1

Pseudo first order degradation rate constants of epi-brassicasterol and 24-methylenecholesterol during in vitro incubations and in Arctic oxic sediments

	$k_{\text{Bra}} \text{ (h}^{-1}\text{)}^{\text{a}}$	r^2	n	$k_{24\text{-Me}} \text{ (h}^{-1}\text{)}^{\text{b}}$	r^2	n
Autoxidation in algal cells (seawater + Fe^{2+}) ^c	2.9×10^{-4}	0.80	4	1.1×10^{-3}	0.85	4
Aerobic biodegradation of algal cells	3.5×10^{-3}	0.95	4	3.6×10^{-3}	0.93	4
Degradation in sediments from station 308 ^d	2.0×10^{-6}	0.86	6	3.3×10^{-6}	0.94	6

^a Pseudo first order degradation rate constant of epi-brassicasterol, ^b Pseudo first order degradation rate constant of 24-methylenecholesterol, ^c Rontani et al. (2014), ^d First 10 cm

- Manuscript OG-3440

- Comment 1: The answer to the first comment of reviewer #2: "Chronologies of these sediments (which also provide bioturbation depths) are in progress and could not be included in the present paper focusing on degradation processes. It is now indicated that an effect of bioturbation processes in the sediments investigated cannot be totally ruled out (see text p. 21-22 lines 479-481). In Figure 3 concentrations of IP25 are now expressed relative to TOC." does indeed provide a sentence naming the term bioturbation ONCE at the far end of the whole manuscript (line 480) and without reference(s). This needs to be expanded because also reviewer #1 was wondering about it and I agree that the answer is not satisfactory. If not (yet) available for the core(s), please provide references that judge to why bioturbation is important (down to which depth?) or can be neglected.

- Answer: Bioturbation was neglected on the basis of previous ^{210}Pb measurements. The following text was added p.22 lines 494-497: "*However, preliminary ^{210}Pb data suggest that bioturbation is negligible in cores from Barrow Strait (STN4) and Viscount Melville Sound (STN308), and confined to the (at most) upper 2 cm in the core from the western Amundsen Gulf (STN408) (S. Schmidt, personal communication).*"

- Comment 2: The authors now express concentrations relative to TOC (Fig. 3) which is good, but should be actually specified in the Figure text. However, it seems that the concentrations are much too high (now is $\mu\text{g} / \text{mg}$ TOC but should rather be $\mu\text{g} / \text{g}$ TOC from what I am generally aware of). This has to be clarified. Representation of the TOC values (if not visible for all cores in the Berben et al., 2017 reference) should be added to supplementary data, so that concentration calculations are reasonable for everyone.

- Answer: There was an error in the TOC unit, which is effectively $\mu\text{g g}^{-1}$ TOC. The figure 3 was changed accordingly and as suggested by the editor a table showing the calculations was added to supplementary data.

- Comment 3: Contrarily to what the authors write in the response, the answer provided to the following comment is not comprehensive: Lines 380-384 (in the original manuscript) and more generally: The lipid profiles observed in the oxic layer of the sediment from station 408 are not discussed. Could authors comment on these profiles showing a decrease in IP25 concentration in the first 2cm of the oxic layer only, and unexpected fluctuations (an increase followed by a decrease) of the Bra/24-Me sterols ratio in the oxic layer? Please directly answer to the question and do not refer to a former response (which was actually a different reviewer comment).

- Answer: The following text was added p.19 lines 419-424: "*In contrast, the strong decrease in Bra/24-Me observed in the bottom of the oxic layer of sediments from the western*

Amundsen Gulf (STN 408) is potentially due to an input of fresh algal material (with a low Bra/24-Me ratio) during this period. This suggestion is supported by the observation of a 10-fold increase in phytoplanktonic sterol concentration in the 6-7 cm horizon compared to the 4-5 cm layer.”

- Comment 4: The response given to the following comment is not fully agreed upon by the reviewer: Lines 358-363 (of the first manuscript): This was observed for cholesterol only and not for 24-methyl (or 24-methylidene) structures. The statement of similar anaerobic biodegradation rate for the two sterols is thus very hypothetical and, as such, cannot be taken for granted. The answer that cholesterol, brassicasterol and 24-methylene cholesterol possess the same cyclic structure and differ only by their side-chain is not conclusive. Since under anaerobic conditions the side-chain is not assimilated, it is actually not expected that similar biodegradation rates of these three sterols have to be taken for granted. Because we do not clearly know whether the side-chain plays a role (is assimilated) or not during the anaerobic biodegradation of sterols since data are scarce (if not, more references could be given). The presence of an extra methyl group and/or of a double bond may significantly influence the degradation pathways. This should be answered more carefully by the authors. I agree. Please provide further background (with references) on this.

- Answer: The following text was added p. 18 lines 390-397: “*For sterols with more substituted or unsaturated side chains, such as sitosterol, fucosterol and isofucosterol, similar degradation rates were observed following incubation of cells of the microalga Nannochloropsis salina in anoxic sediment slurries (Grossi et al., 2001). This suggests that changes to the sterol side chain have little impact on the overall degradation rates under anoxic conditions. As such, in the absence of any reported experimental data, it is reasonable to propose similar anaerobic degradation rates for epi-brassicasterol and 24-methylenecholesterol, especially given their common ring structure.*” The reference Grossi et al. (2001) was added in the reference list.

- Comment 5: The final paragraph (4.4 Implications for palaeo sea ice reconstruction) is obviously showing a striking difference in English style (much better) in comparison to the rest of the manuscript. I recommend that the rest of the manuscript is re-checked carefully in this direction by all members of the author's team.

- Answer: All the text was carefully checked by Dr. S.T. Belt.

